UNIVERSITAT POLITÈCNICA DE CATALUNYA
BARCELONATECH
Escola Superior d'Enginyeries Industrial,
Aeroespacial i Audiovisual de Terrassa

Study and structural analysis of a monocoque wing with composite materials for a model aircraft

BACHELOR'S DEGREE THESIS

Bachelor's degree in Aerospace Vehicles Engineering

DOCUMENT 1. REPORT

Albert Herrando Moraira

Director: Lluís Gil Espert

June 2017

Universitat Politècnica de Catalunya

Escola Superior d'Enginyeries Industrial, Aeroespacial i Audiovisual de Terrassa

"Every great dream begins with a dreamer. Always remember, you have within you the strength, the patience, and the passion to reach for the stars to change the world."

Harriet Tubman (1822-1913)

Acknowledgements

First of all, I would like to thank Professor Lluís Gil Espert for guiding me through the development of my Bachelor's degree thesis and for his expert advice when difficulties came up. He has always been truly kind and supporting.

Secondly, I would like to express my gratitude to my team mate and friend Gurinder Saran. We both have been doing our thesis during this time and we have spent lots of working hours together. For your company through the good and bad moments and your positive energy, thank you.

I am also grateful to Trencalòs Team and all its members. Being part of this team has been deeply gratifying and I really appreciate the help of the simulations department formed by Càndia Muñóz Tardà and Joan Altimira Marfà.

Finally, this project could not has been possible without the support of my family and friends. Thank you all very much for being with me through this research and let me accomplish my dreams.

Abstract

Trencalòs Team is a research team mainly formed by aeronautical engineers who are specialized in aeromodelling. They organize several activities in *The School of Industrial, Aerospace and Audiovisual Engineering of Terrassa (ESEIAAT)* in order to divulge knowledge of aeronautics and to improve the relation between the students and the university.

Its main activity is to participate to an international competition called Air Cargo Challenge. It consists of manufacturing and flying a model aircraft capable of lift up as much payload as possible while performing a circuit.

For the Air Cargo Challenge 2017 event, the team decided to take the plunge and bring a new aircraft concept. It consisted of a monocoque wing structure made of composite materials. This thesis is focused on finding an optimum design that could compete with aircraft from all around the world.

To do so, an iterative design process has been carried out. Using Abaqus, a Finite Element Method (FEM) software, different cases of structures have been analyzed. In the end, the best design has been selected and it is the one that Trencalòs Team will bring to the Air Cargo Challenge 2017.

Summary

This thesis is divided in three documents and one DVD which are described below.

Document 1. Report

The report corresponds to this document and it presents the work that has done during the development of the study. It is divided into the following parts:

- **Chapter 1. Introduction:** A summary of the aim, scope and objectives is presented beside the justification and the planning of the study.
- **Chapter 2. State of the art:** An explanation of the Air Cargo Challenge competition and of the role of Trencalòs Team in this event are delivered.
- **Chapter 3. Premises of the design:** The initial features of the design are detailed, including geometries, structural elements, materials and structural requirements.
- **Chapter 4. Failure criteria and Pareto efficiency:** The methodology that allows the user to chose which are the optimal designs is presented.
- **Chapter 5. Design process description:** All the necessary steps from the beginning to the final design are explained in this chapter.
- **Chapter 6. Starting point designs:** The design process is applied to a first batch of cases and some conclusions are obtained.
- **Chapter 7. Improved designs:** Based on the results of the previous chapter, a second batch of cases that include several improvements is analyzed.
- **Chapter 8. Conclusions:** With all the information of the thesis, some conclusions about the software, the design process and the final design are detailed.
- **Future work:** The possible improvements and the future continuity of the thesis are presented.

- **Environmental and security impact:** An insight of the environmental impact and the security measures of this thesis are commented.
- **Bibliography:** All the references that have been used while developing this work are attached.

Document 2. Annexes

The annexes contain extra information of the thesis which it is organized as follows:

- **Chapter 1. Skin options:** The possible skins combinations that could have been used are presented in a table.
- **Chapter 2. Scripts and utilities:** The codes developed in Python and Matlab languages to carry out the analysis are attached.
- **Chapter 3. Numerical results:** All the results of the simulations, of both the initial cases and the improved ones, have been tabulated.

Document 3. Budget

In this document, the budget of the implementation of the thesis in a real business is attached. Its information is classified in:

- **Professional fees:** The cost of the hours of a junior engineer working on the thesis are accounted in this section.
- **Implementation cost:** The material and software prices have been summarized.
- **Budget bibliography:** The references used for the budged have been attached.

DVD

All the files of the thesis have been burned into a DVD. It includes the electronic documents in PDF format, the images that have been used and all the simulations and scripts that have been developed.

This DVD has been handed out to the director of the thesis, to the *Department of Strength of Materials and Structural Engineering* of *The School of Industrial, Aerospace and Audiovisual Engineering of Terrassa (ESEIAAT)* and to Trencalòs Team.

Contents

List of Figures

List of Tables

List of abbreviations

ACC2017	Air Cargo Challenge 2017
MTOW	Maximum take off weight
MSTRS	Maximum stress theory failure measure
MSTRN	Maximum strain theory failure measure
TSAIH	Tsai-Hill theory failure measure
TSAIW	Tsai-Wu theory failure measure
AZZIT	Azzi-Tsai-Hill theory failure measure
HSNFTCRT	Hashin's fiber tensile damage initiation criterion
HSNFCCRT	Hashin's fiber compressive damage initiation criterion
HSNMTCRT	Hashin's matrix tensile damage initiation criterion
HSNMCCRT	Hashin's matrix compressive damage initiation criterion
BTCRT	Beam tensile damage initiation criterion
BCCRT	Beam compressive damage initiation criterion
BSHCRT	Beam shear damage initiation criterion
ERParalTCRT	End rib parallel tensile damage initiation criterion
ERPerpenTCRT	End rib perpendicular tensile damage initiation criterion
ERParalCCRT	End rib parallel compressive damage initiation criterion
ERPerpenCCRT	End rib perpendicular compressive damage initiation criterion
ERSHCRT	End rib shear damage initiation criterion
XFLR5	Low Reynolds software for airfoils and planes
CFAILURE	All failure measure components
E	All strain components
P	Uniformly distributed pressure load on element faces
RF	All components of reaction forces
S	All stress components
U	All physical displacement components
FRP	Fibre-reinforced plastic
CF	Carbon fiber
UD	Unidirectional

List of symbols

λ	Buckling eigenvalue
E	Elastic modulus or Young's modulus
G	Shear modulus or modulus of rigidity
ν **or** μ	Poisson's ratio
Xt	Ultimate tensile strength parallel to the fiber
Xc	Ultimate compressive strength parallel to the fiber
Yt	Ultimate tensile strength perpendicular to the fiber
Yc	Ultimate compressive strength perpendicular to the fiber
S	Ultimate in-plane shear strength
$X\varepsilon t$	Ultimate tensile strain parallel to the fiber
$X\varepsilon c$	Ultimate compressive strain parallel to the fiber
$Y\varepsilon t$	Ultimate tensile strain perpendicular to the fiber
$Y\varepsilon c$	Ultimate compressive strain perpendicular to the fiber
$S\varepsilon$	Ultimate in-plane shear strain
D	Parameter of the orthotropic stiffness matrix
L	Total lift of the aircraft
W	Weight of the aircraft
n	Load factor
θ	Bank angle
σ	Stress
ε	Strain

Chapter 1

Introduction

1.1 Aim

The purpose of this thesis is to design a monocoque structure with composite materials for a model aircraft wing. In order to accomplish such an objective, it was necessary to use a Finite Element Method (FEM) software which works with composite materials. The final design is going to be the one which will participate to the Air Cargo Challenge 2017 competition on behalf of Trencalòs Team.

1.2 Scope

The scope of the study was divided into different sections:

- **Information research**
  - **Precedents:** This thesis is an application of a previous one called *Study and design of a monocoque wing structure with composite materials* [15] by Miguel Alejandro Pareja Muñoz. Its methodology was studied and considered strongly.
  - **Abaqus CAE:** This is the main software the thesis used and its performance was studied. From the basics to the use of composite materials in its simulations.
- **Software learning**
  - **Abaqus CAE:** In order to design the monocoque wing the following fields of this software were studied: basic concepts, finite element types and applications, standard and explicit analysis, meshing techniques, composite materials and different simulations.

  - **CATIA V5R20:** This program was used to define the geometry and to import it to Abaqus CAE.

- **Technical design**

  - **Design premises:** This section includes the wing geometry, the structural elements that were used, the materials and their properties, the structural requirements and the design parameters.
  - **Design process description:** Its parts are the initial tests, the starting design point, the possible improvements, the selection criteria that's going to be used during the analysis and the final design process. This one is an iterative process where an improvement of each model is done.
  - **Analysis process:** It consists of the pre-processing of the model, the analysis simulation and the post-processing.
  - **Analysis of the results:** Once all the analysis were finished, the discussion of the results and the decision of the final design were determined.

- **Conclusions**

  - **Software conclusions:** The experience as an Abaqus CAE and CATIA V5R20 user is explained.
  - **Design process conclusions:** The advantages and drawbacks of the chosen method are discussed.
  - **Final design conclusions:** The reasons why the final wing structure has been selected are exposed.

- **Deliverables**

  - **Report:** It is the main document of the thesis which includes all the work done.
  - **Annexes:** Not required document which can consist of extra information or extra work.
  - **Budget:** Document that includes the price that the project would cost if it's wanted to be done.
  - **Presentation:** It's an oral presentation in front of an academic jury where the thesis is explained.

1.3 Requirements

To achieve the goal of the thesis the following requirements were fulfilled:

- **Technical requirements**
  - The wingspan of the design had to be 4 meters.
  - The composite materials used had to be fibrous based with an epoxy matrix.
  - The structure had to bear the aerodynamic loads of the aircraft.
  - The wing had to be demountable into 5 parts in order to fulfill the competition requirements.
- **Economical requirements**

  As an academic study, this thesis does not have a specific economical limit. However, the reader can find its budget in the Document 3. Budget. It gives an idea of the costs that would involve the execution of this study in a business environment.

1.4 Justification

1.4.1 Identification of the need

Trencalòs Team is a group of students of aeronautical engineering from the *Polytechnic University of Catalonia*, specifically from *The School of Industrial, Aerospace and Audiovisual Engineering of Terrassa, ESEIAAT*. The aims of the team are to divulge aeronautical knowledge, organize activities that strengthen the relation between the university and the students, motivate people and help them to develop engineering skills.

To do so, the team carries out formative talks, organizes airplanes competitions and builds model airplanes right from the start. Trencalòs Team funding is possible thanks to the university and its INSPIRE program and to the sponsors that give materials, tools and other facilities.

The main objective of the team is to participate in a competition called Air Cargo Challenge. It is an international event where groups of engineers have to manufacture and flight model aircraft with specific features. It is explained in chapter 2 with more details. Trencalòs has participated in it since 2007 and the next one is in 2017, so it has become a tradition. In section 2.2 a brief explanation of each year is going to be presented.

During 2016, two members of the team had to do their bachelor's degree thesis [15, 2] and they decided to study the application of composite materials in model aircraft.

For Air Cargo Challenge 2017, the team needed a new aircraft to compete and it was decided to take advantage of the previous studies to bring an airplane made of composite materials. So the main motivation of this current thesis came because the team had the necessity to design a new concept of structure for the aircraft.

1.4.2 Usefulness of the study

This thesis has several uses. Firstly, the obtained results will serve to set a structural design for the next ACC 2017 competition. What is wanted is to determine a structure for the wing that bears the necessary loads while is made of composite materials.

On the other hand, the study will be a tool for Trencalòs Team that will allow the development of future structural designs using Abaqus. For instance, it could be used in Air Cargo Challenge 2019 or in some model aircraft that the team wants to manufacture.

Finally, the acquired knowledge could be divulged so as to other engineering students could learn how to use this tool. Even formative talks of Abaqus could be carried out in a future.

1.5 Study's approach

The objective of the thesis is to find a wing structure that carries the necessary flight loads. The wing surface has to be made of composite materials forming a structural skin which bears the majority of the forces. It has to be lightweight and stiff at the same time.

To approach this goal certain tasks has to be done. The study will start with an information research and a software learning. Then, the premises of the design will be studied. They include the wing features, the structural elements that can be used, the materials and the structural requirements that are needed.

After that, the designing criteria will be set and the design process defined. Once done, a first batch of designs will be analyzed, extracting some conclusions from them. It will serve to set a second batch of structures that will bring improvements. They will be simulated and the final conclusions will be obtained.

1.6 Planning

In order to achieve the goal of this thesis, the work that had to be completed was divided into work packages. The tasks explained in the scope section were broken down into sub-tasks and they were coded respectively. The Table 1.1 shows the task codes, their name and if there are some other task that had to be completed to start them.

Once identified the work packages and their tasks, the calendar was organized so as to complete them all. A Gantt diagram, which can be seen in Figure 1.1, was done to see the tasks through the time and its dates are shown in detail in the Table 1.2.

In the next pages it is possible to observe the starting and ending dates beside a Gantt diagram which shows the duration and inter-dependency of the tasks.

Code of task	Task identification	Preceding task
I	Information research	
I.1	Precedents	
I.2	Finite element programs	
I.3	Abaqus CAE	
I.3.1	Basics	
I.3.2	Finite Elements	I.3.1
I.3.3	Materials	I.3.1
I.3.4	Theories	I.3.1
S	Software learning	
S.1	Abaqus CAE	
S.1.1	Basic concepts	
S.1.2	Finite element types and applications	S.1.1
S.1.3	Standard and explicit analysis	S.1.1
S.1.4	Meshing	S.1.1
S.1.5	Composite materials in Abaqus CAE	S.1.1
S.1.6	Simulation of examples	I.3.2 - I.3.3 - I.3.4 - S.1.2 - S.1.3 - S.1.4 - S.1.5
S.2	CATIA V5R20	
S.2.1	Geometry definition	
S.2.2	Importation and exportation with Abaqus CAE	
T	Technical Design	
T.1	Design premises	I - S
T.2	Design process description	T.1
T.3	Analysis process	T.2
T.4	Analysis of the results	T.3
C	Conclusions	
C.1	Software conclusions	T
C.2	Design process conclusions	T
C.3	Final design conclusions	T
D	Deliverables	
D.1	Project charter (03/03/2017)	I.1
D.2	Follow-up 1 (31/03/2017)	
D.3	Follow-up 2 (28/04/2017)	
D.4	Follow-up 3 (24/05/2017)	
D.5	Delivery (10/06/2017)	I - S - T - C
D.5.1	Report writing-1	I - S
D.5.2	Report writing-2	D.5.1 - T - C
D.5.3	Annexes and budget	D.5.1 - T - C
D.6	Presentation (26/06/2017)	D.5
D.6.1	Presentation realization	D.5
D.6.2	Presentation preparation	D.6.1

Table 1.1: Relation between tasks. Each task is identified with a code and the preceding ones are indicated.

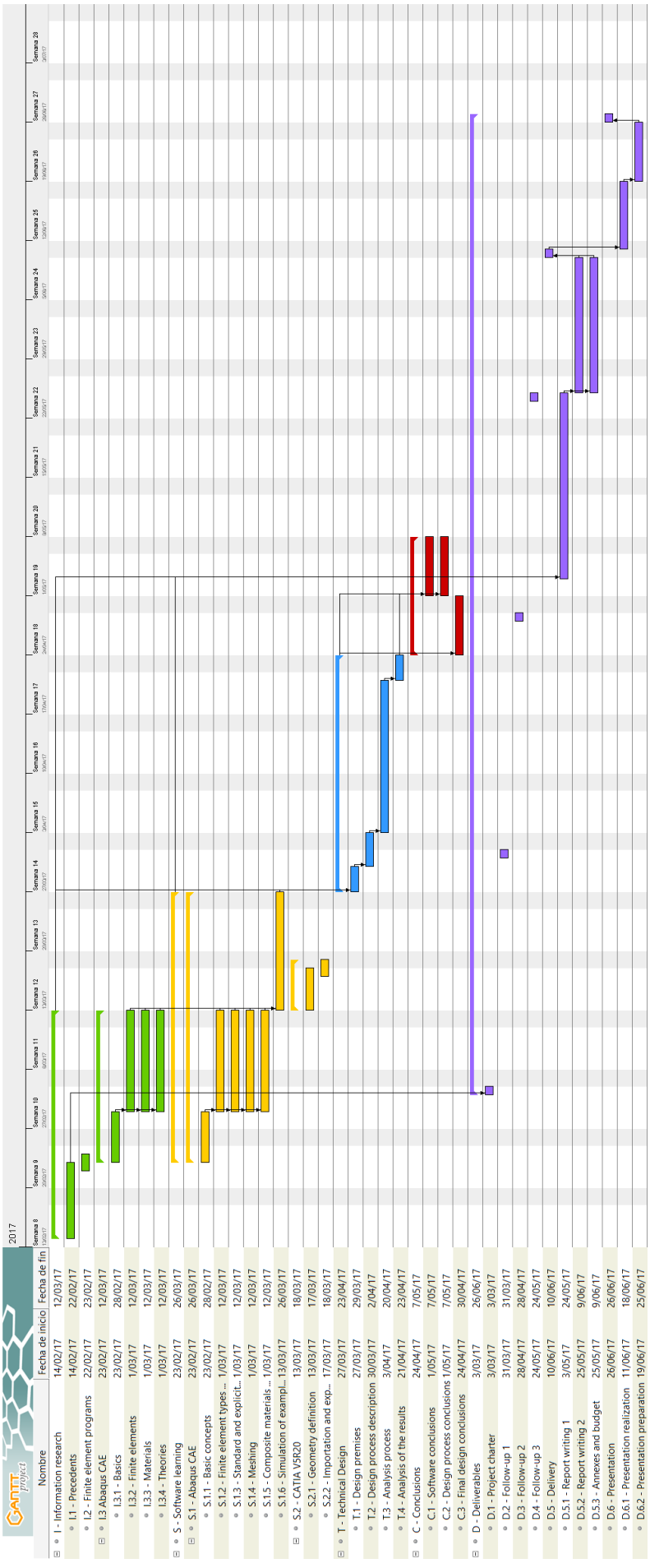

Figure 1.1: Gantt diagram of the study.

Task	Start date	Ending date
I - Information research	14/02/2017	12/03/2017
I.1 - Precedents	14/02/2017	22/02/2017
I.2 - Finite element programs	22/02/2017	23/02/2017
I.3 Abaqus CAE	23/02/2017	12/03/2017
I.3.1 - Basics	23/02/2017	28/02/2017
I.3.2 - Finite elements	01/03/2017	12/03/2017
I.3.3 - Materials	01/03/2017	12/03/2017
I.3.4 - Theories	01/03/2017	12/03/2017
S - Software learning	23/02/2017	26/03/2017
S.1 - Abaqus CAE	23/02/2017	26/03/2017
S.1.1 - Basic concepts	23/02/2017	28/02/2017
S.1.2 - Finite element types and applications	01/03/2017	12/03/2017
S.1.3 - Standard and explicit analysis	01/03/2017	12/03/2017
S.1.4 - Meshing	01/03/2017	12/03/2017
S.1.5 - Composite materials in Abaqus CAE	01/03/2017	12/03/2017
S.1.6 - Simulation of examples	13/03/2017	26/03/2017
S.2 - CATIA V5R20	13/03/2017	18/03/2017
S.2.1 - Geometry definition	13/03/2017	17/03/2017
S.2.2 - Importation and exportation with Abaqus CAE	17/03/2017	18/03/2017
T - Technical Design	27/03/2017	23/04/2017
T.1 - Design premises	27/03/2017	29/03/2017
T.2 - Design process description	30/03/2017	02/04/2017
T.3 - Analysis process	03/04/2017	20/04/2017
T.4 - Analysis of the results	21/04/2017	23/04/2017
C - Conclusions	24/04/2017	07/05/2017
C.1 - Software conclusions	01/05/2017	07/05/2017
C.2 - Design process conclusions	01/05/2017	07/05/2017
C.3 - Final design conclusions	24/04/2017	30/04/2017
D - Deliverables	03/03/2017	26/06/2017
D.1 - Project charter	03/03/2017	03/03/2017
D.2 - Follow-up 1	31/03/2017	31/03/2017
D.3 - Follow-up 2	28/04/2017	28/04/2017
D.4 - Follow-up 3	24/05/2017	24/05/2017
D.5 - Delivery	10/06/2017	10/06/2017
D.5.1 - Report writing 1	03/05/2017	24/05/2017
D.5.2 - Report writing 2	25/05/2017	09/06/2017
D.5.3 - Annexes and budget	25/05/2017	09/06/2017
D.6 - Presentation	26/06/2017	26/06/2017
D.6.1 - Presentation realization	11/06/2017	18/06/2017
D.6.2 - Presentation preparation	19/06/2017	25/06/2017

Table 1.2: Duration of the tasks. The starting and ending dates of each one are shown.

Chapter 2

State of the Art

2.1 The Air Cargo Challenge competition

The Air Cargo Challenge (ACC) is an aeronautical engineering competition where students from universities of all the world can apply their theoretical knowledge and develop practical skills. It is celebrated every two years in different countries and until now it has always been organized in Europe.

The objective is to build a radio-controlled aircraft which can carry the highest payload as possible. To achieve this, the teams have to design and manufacture their own plane according to the specifications of the competition [16].

The rules of each competition can vary, however, the aim is the same. For instance, in one competition the wingspan can be limited and in another not.

The order of team winners is based on a certain score. In this punctuation not only is included the fly performance demonstrated, but also a technical report and an oral presentation that shows the quality of the project.

The first competition was organized in 2003 and it was founded by the APAE: Associação Portuguesa de Aeronáutica e Espaço (Portuguese Association of Aeronautics and Space), an aerospace group from Instituto Superior Técnico. They were inspired by the north-American competition Design/Build/Fly. Since Air Cargo Challenge 2007 the competition became international thanks to EUROAVIA, the European Association of Aerospace Students.

Since then, the event is organized by the winner of the past competition and all the teams

have to travel to the host country. Below, there is the list of organizers and the winners.

- 2003 - Organization: APAE, Lisbon

Place	Team	University	Country/City
1º	UBI 2	Universidade da Beira Interior	Covilhã
2º	Flamingo	Universidade do Minho	Guimarães
3º	Beluga	Universidade da Beira Interior	Covilhã

Figure 2.1: ACC 2003 winners. Extracted from [1].

- 2005 - Organization: APAE, Lisbon

Place	Team	University	Country/City
1º	Ícaro	Instituto Superior Técnico e Universidade de Coimbra	Lisboa/Coimbra
2º	Fly By	Faculdade de Engenharia da Universidade do Porto	Porto
3º	Pegasus	Universidade da Beira Interior	Covilhã

Figure 2.2: ACC 2005 winners. Extracted from [1].

- 2007 - Organization: Instituto Superior Técnico, Lisbon

Place	Team	University	Country
1º	PEGASUS II	Universidade da Beira Interior	Portugal
2º	Akamodell Stuttgart	Universidade de Estugarda	Germany
3º	Blei-Ente	Euroavia Muenchen	Germany

Figure 2.3: ACC 2007 winners. Extracted from [1].

- 2009 - Organization: University of Beira Interior, Covilhã

Place	Team	University	Country
1º	Akamodell Stuttgart	Universidade de Estugarda	Germany
2º	TU Heavy	Universidade Técnica de Munique	Germany
3º	ESTG Cargo2	Instituto Politécnico de Leiria	Portugal

Figure 2.4: ACC 2009 winners. Extracted from [1].

- 2011 - Organization: University of Stuttgart, Stuttgart

Place	Team	University	Country
1º	UBI - Portugal	Universidade da Beira Interior	Portugal
2º	TU Eleven	Universidade Técnica de Munique	Germany
3º	Universidade de Tsinghua	Universidade de Tsinghua	China

Figure 2.5: ACC 2011 winners. Extracted from [1].

- 2013 - Organization: University of Beira Interior, Lisbon

Place	Team	University	Country
1º	AKAModell Stuttgart e.V.	Universidade da Estugarda	Germany
2º	Tsinghua University	Universidade de Tsinghua	China
3º	Beihang Aeromodelling Team 1	Universidade de Beihang	China

Figure 2.6: ACC 2013 winners. Extracted from [1].

- 2015 - Organization: University of Stuttgart, Stuttgart

Place	Team	University	Country
1º	EUROAVIA Zagreb	Universidade de Zagreb	Croatia
2º	Born TU Lift	Universidade Técnica de Munique	Germany
3º	EUROLIFTER	Universidade de Tecnologia de Rzeszów	Poland

Figure 2.7: ACC 2015 winners. Extracted from [1].

In 2015, the team EUROAVIA Zagreb won the event so this 2017 the ACC will be carried out in Zagreb, Croatia. All the information, requirements, deadlines, programs, etc. can be found in their official web page [16].

2.2 Structures and materials of past years

The first time that Trencalòs Team participated to the ACC competition was in 2007. Since then, every two years the team has compete with a different plane.

The following sections show the aircraft that were presented with some explanations about the type of structures that they had and which materials they used.

2.2.1 ACC 2007, Lisbon

Regarding the first ACC, Trencalòs Team ventured to design a biplane model. As can be seen in Figure 2.8b, it was composed by two wings in different heights from the ground. The lead one was lower than the rear one so as to avoid airflow interference.

The structure of the wing was simple. Figure 2.8a shows a core of expanded polystyrene covered with balsa wood and painted. There weren't neither spars nor ribs inside the wing.

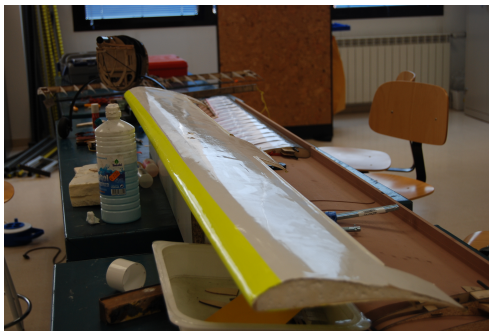

(a) Wing detail

(b) Aircraft

Figure 2.8: ACC 2007 structure. Extracted from Trencalòs Team.

2.2.2 ACC 2009, Covilhã

In ACC 2009 the aircraft concept changed. The biplane was discarded because of its bad aerodynamic efficiency. So the plane evolved to a design with a conventional wing and a T empennage as Figure 2.9b shows. It is also noticeable that the fuselage adopted a simpler solution using a carbon fibre tube.

The inner structure wing also experimented big changes. A spar was incorporated to bear the loads and balsa wood ribs shaped the airfoil profile. To ensure enough strength, the lead part of the wing was reinforced with a layer of polyamide and carbon fiber. Then the rear part was covered with a light-weight plastic called Oracover or Ultracote.

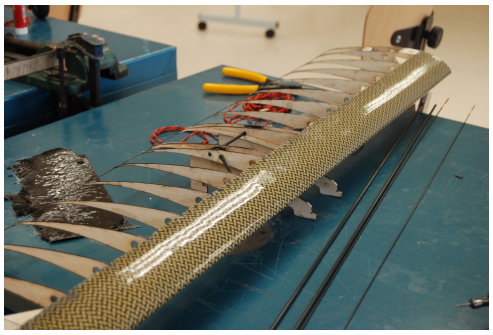

(a) Wing detail

(b) Aircraft

Figure 2.9: ACC 2009 structure. Extracted from Trencalòs Team.

2.2.3 ACC 2011, Stuttgart

During the ACC 2011 competition there was not much innovation regarding the design. The same idea from the past event was used, including a spar, balsa wood ribs, and the lead reinforcement.

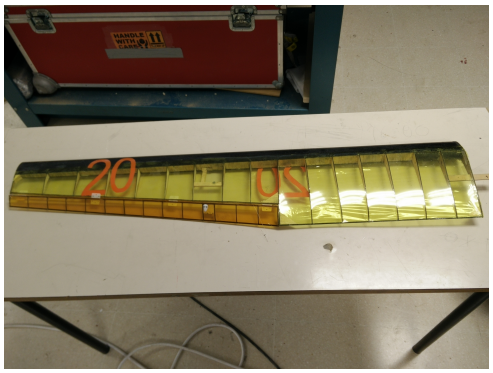

(a) Wing detail

(b) Aircraft

Figure 2.10: ACC 2011 structure. Extracted from Trencalòs Team.

2.2.4 ACC 2013, Lisbon

In this edition the organizers decided to make considerable changes in the regulations. The biggest one was that there was no wingspan limit. For that reason, the dimensions of the aircraft that the team carried were substantial.

Figure 2.11b shows that the body configuration was also changed. There were two carbon tubes that constituted the fuselage and an empennage with a double fin.

On the other hand, the wing structure experimented modifications. It was the first time that a closed-cell rigid foam based on polymethacrylimide was used. This material is known as Rohacell 31 IG-F and was the replacement of the previous balsa wood spar.

Apart from that another material was introduced: the birch wood. It is a lightweight and resistant wood that was used in the ribs. The lead carbon reinforcement was still applied and the rear part was covered with Oracover.

The use of birch wood for the ribs turned out to be a big mistake. Despite the fact that the aircraft was really tough, its weight increased so much that it had a lot of trouble flying.

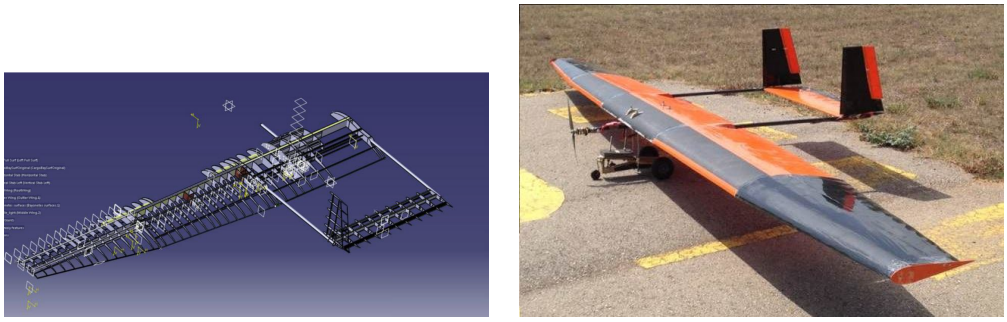

(a) Wing detail (b) Aircraft

Figure 2.11: ACC 2013 structure. Extracted from Trencalòs Team.

2.2.5 ACC 2015, Stuttgart

After the experience of the ACC 2013 with a heavy plane, in the 2015 edition, it was seriously taken into account the factor of the aircraft weight. This had a huge effect in the design presented.

The team implemented a conventional aircraft but with a completely new concept. It had a high-wing configuration, with a slender fuselage and a conventional empennage.

The biggest innovation was in the inner wing structure which is possible to observe in Figure 2.12a. It was made of a milled block of Rohacell 31 IG-F with the wing shape including holes to decrease the weight. In order to bear the bending moment carbon stringers were added to increase the strength of the structure. Finally it was covered up with Oracover.

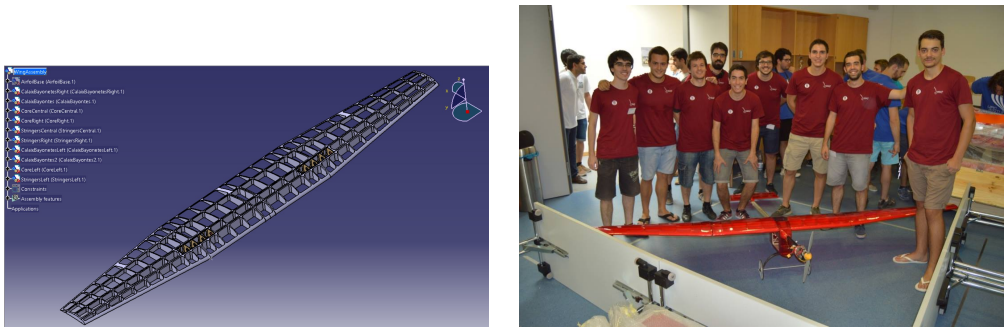

(a) Wing detail (b) Aircraft

Figure 2.12: ACC 2015 structure. Extracted from Trencalòs Team.

2.3 Next step: Structural skin with composite materials

After the Air Cargo Challenge 2015, the next year there was not competition. During that time, two bachelor thesis where carried out in Trencalòs Team related with composite materials [15, 2]. They studied a small rectangular wing made of glass and carbon fiber. These studies supposed a first step and iteration to the world of model aircraft made of composites.

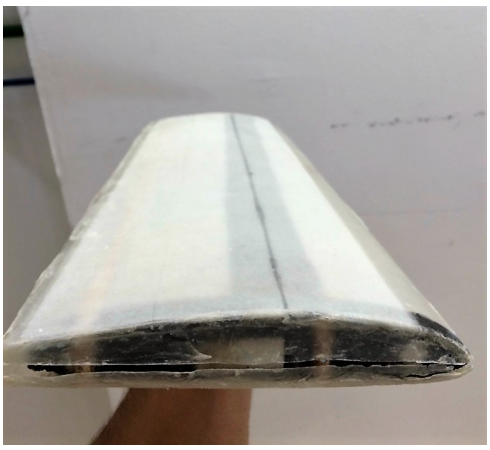

Figure 2.13: Composite wing manufactured by Trencalòs Team. Extracted from [2].

Taking advantage of this work, in 2017 Trencalòs Team decided to take the plunge and bring a composite wing. In the 2015 edition, the best designs were made of composites so in order to compete the team had to apply this technology.

2.4 Structural design nowadays

When a wing structure is designed there are several tools to be used. The classical manual calculations based on the strength of materials theories can be used. But with them, just simple cases can be analyzed and various approximations have to be done which, in the end, differ from the reality.

The other option is the use of numerical methods. They are based on the discretization of a model and the application of the fundamental equations in every resulting node. These procedures are nowadays implemented in some software. There are lots of them and each one has its own application. Generally, we can classify them into commercial and open source software.

Commercial software: Abaqus [17], ANSYS [18], COMSOL [19], NASTRAN [20], Autodesk Simulation [21], SolidWorks Simulation [22], etc.

Open source software: Code_Aster [23], Calculix [24], etc.

In this thesis, the Abaqus software [17] was decided to be used because Trencalòs Team had already acquired some experience in its use.

Chapter 3

Premises of the design

To find the best design of a wing structure using composite materials and other structural elements it is necessary to optimize lots of parameters. Approach them all would take a long time and a high knowledge of programming and materials engineering would be required.

For this reason, part of the geometrical parameters and some materials were fixed. The premises of the design will be explained in the following sections.

3.1 Wing's geometry

The geometry of the wing is based in three determining factors:

- **Aerodynamics:** The aerodynamics department of Trencalòs Team determined the airfoil of the wing and its planform iterating so as to get the maximum punctuation possible with the aircraft MTOW. They achieved a wing with a NACA 6314 airfoil and with 4 metres of wingspan including tapered endings.
- **The travel box:** The Air Cargo Challenge 2017 competition [25] impose that the plane has to fit into a box which sizes are 1x0.5x0.4 metres. It will be invoiced in the flight from Barcelona to Zagreb. Thus, with a wingspan of 4 metres, there were two options: cut the wing into four or five parts. In the end the second option was chosen because in this way the central part (which is the one that is joined with the fuselage and bear the maximum tensions due to the bending moment) was stiffer.
- **Construction process:** The main objective was the use the smallest possible number of molds in order to speed up the construction of the wing.

The resulting wing geometry was the one shown in Figure 3.1.

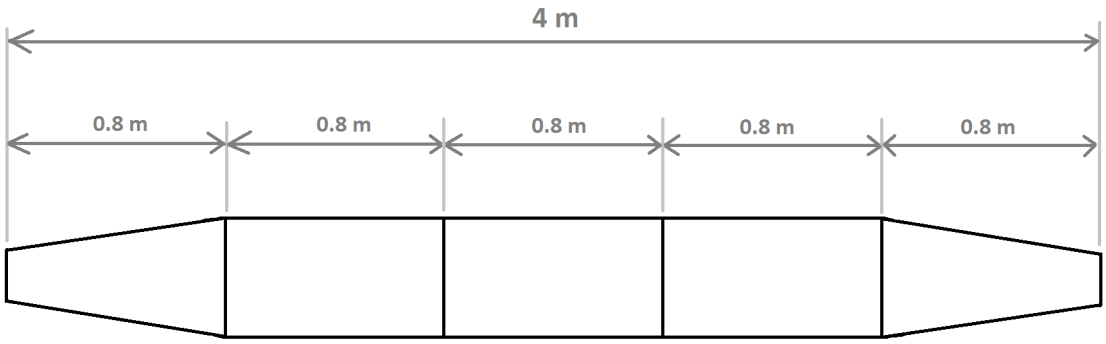

Figure 3.1: Wing planform of the Trencalòs Team airplane for ACC 2017.

At this point, the flaps and ailerons had to be incorporated to the design. It was decided that both the flaps and the ailerons would occupy all the trailing edge of the wing. This was done to make easier the construction with molds and composite materials. If it was not done in this way, there would have been right angles which would have led to a difficult lamination process.

So the wing will consist of three central parts with the same geometry and two parts at the ends. Figure 3.2 shows the design. Note that six moulds will be needed to manufacture all the skins. The extradoses and intradoses are split because the construction method uses female moulds to laminate the skin. For more details, the reader can consult the manufacturing process in the following references [3] and [2].

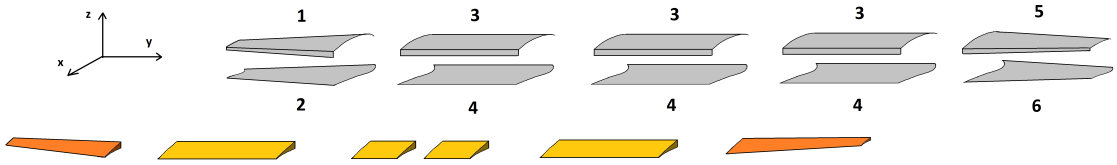

Figure 3.2: Preliminary parts of the wing.

Once the geometry of the wing was set the servos had to be considered to move the control surfaces. They had to be removable in case they break. There were different options regarding their position which are illustrated in Figure 3.3.

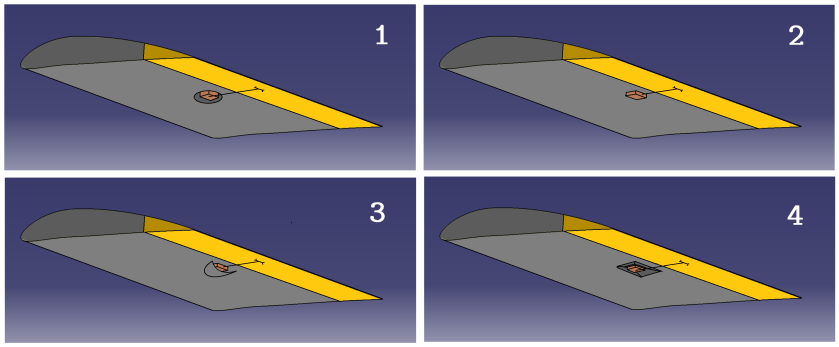

Figure 3.3: Possible positions of the servos on the intrados.

- **Option 1:** Pierce the structural skin and put them into the wing.
- **Option 2:** Place the servos on the intrados using glue.
- **Option 3:** The same as option 2 but including a fairing which enhance the aerodynamics.
- **Option 4:** Manufacture a wing with a sinking which allow the servo be positioned in it.

With this alternatives, another decision had to be done. The first option was discarded because the fact of piercing the wing would have caused high tensions around the hole. The last one was rejected because its difficulties during the manufacturing process and the possible tensions that a sinking would have provoked. Finally, between options two and three the third one was chosen because it generated less drag.

When all of these decisions were made, the geometry of the wing was already fixed. Five parts were forming the wing, three of them equal and without taper and two with taper at the ends. What was still remaining was the design which joined the parts and the inner elements that allowed the wing to bear the loads.

3.2 Structural elements

In this section, the structural elements that were considered to use are presented. Using them wisely would lead us to a wing design capable of resist the necessary forces.

3.2.1 Skin

As it was explained in section 2.3, Trencalòs Team wanted to bring an aircraft made of composite materials. Then it was decided that the wing could be formed by a structural

skin which is a stack of various composite layers. Based on other studies [15], a sandwich structure was chosen.

This designs has interesting features. They are manufactured attaching two thin layers of composites on a thick core. The outer layers provide the necessary stiffness while the core is made of a lightweight material which gives a high bending stiffens without increasing the weight of the structure so much. The reader can see a representation in Figure 3.4.

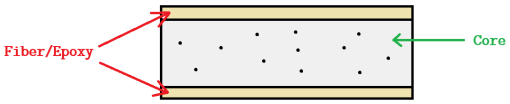

Figure 3.4: Representation of a structural skin made of a sandwich design.

With regard to the thin composite layers, they can be made of various materials (explained in section 3.3) and configurations. Depending on them the laminate has different properties.

The direction of the fibers is a crucial parameter that affects to the final performance of the structure. There are lots of configurations but the most common ones are the unidirectional fibers and the perpendicular fabrics shown in Figure 3.5.

Figure 3.5: Fabric and unidirectional fibers representation.

In this thesis, the nomenclature of the composite layers directions are expressed as the following example: (0/core/0|90).
The blue and red colors represent the carbon fiber and glass fiber materials respectively. All the orientation angles are measured from the wingspan line so a 0 angle is a unidirectional fiber through the wingspan direction. The 0|90 notation means that is a fabric layer whose fibers are positioned parallel and perpendicular to the wingspan. And finally, the first layer is the inner one and the last layer is the outer.

3.2.2 Spar

In aeronautics, the spars are structural members of a wing that bear flight loads and the weight of the wing. They serve also as a connection point between ribs and a possible structural skin.

During the Air Cargo Challenge 2015 competition, Trencalòs Team carried out some structural tests [26] to get the best design. In their case the spar had to bear all the forces because they did not use a composite skin. In Figure 3.6 different configurations of spars can be seen.

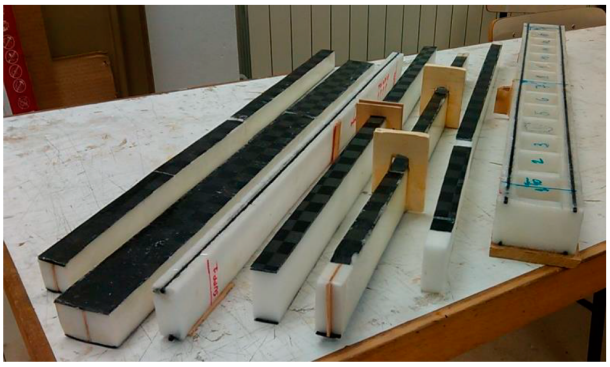

Figure 3.6: Air Cargo Challenge 2015 spar tests. Extracted from Trencalòs Team.

After that, they found that the best design was a double spar structure with holes with four carbon stringers. It correspond to the right spar of the previous figure. Using it was considered but finally discarded because it was too heavy. In our composite design, the skin was the one which had to bear the loads and the spar was simply a reinforcement to transmit the shear forces.

Taking the weight of the models into account, it was decided that the spars would be simple rectangles of Rohacell foam (presented in section 3.3).

3.2.3 Ribs

Ribs are traditional forming elements of the aircraft wing structure. They have the shape of the airfoil and are positioned at frequent intervals through the wingspan. Their function is to ensure that the skin does not bend and to distribute the stresses created by the loads.

The first idea was not to use them because a monocoque design was wanted to perform. But in chapter 7 we will see that in the end they were needed.

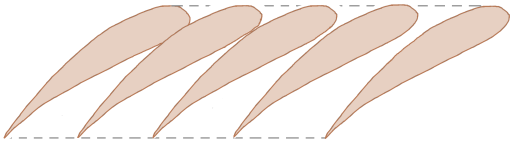

Figure 3.7: Ribs representation.

3.2.4 Load transmission drawers and bayonets

In section 3.1 it was explained that the wing was divided into five parts. Even so, it had to be mounted and had to endure the forces during the flight. Therefore a mechanical union had to be designed.

There were three main loads to transmit from part to part. The first one was the bending moment, and the remaining were the axial, shear, and torsion forces. The team decided to use the concept from the previous Air Cargo Challenge competition [26] shown in Figure 3.8.

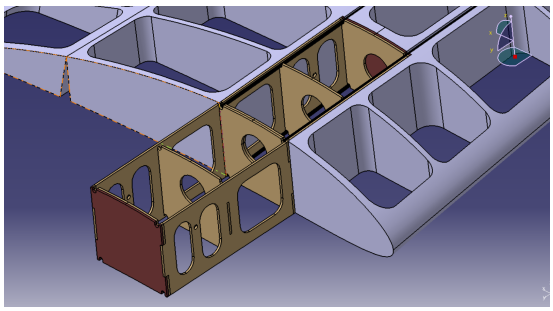

Figure 3.8: Load transmission drawer design from ACC 2015. Extracted from Trencalòs Team.

It consists of a pair of drawers made of birch wood that were placed at the end of two parts to join. Then a hollowed carbon bar was introduced through the drawers and it transmitted the bending moment and the shear forces. The torsion and axial forces were born by four screws. This year, the mechanical design of Figure 3.9 has been set up.

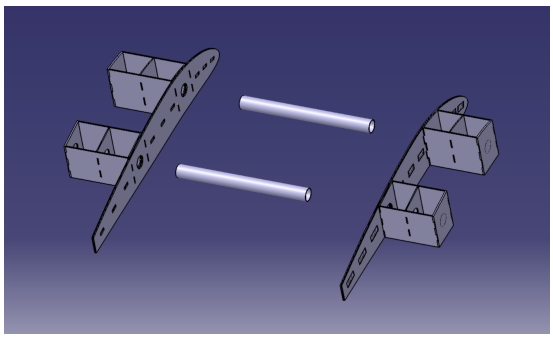

Figure 3.9: Load transmission drawer for ACC 2017. Extracted from [3].

The idea is similar to the previous one with some changes. The problem that the team had was that the structural skin could not be perforated. The four screws were inside the wing so without piercing it they were inaccessible. To solve this issue, two pairs of drawers and two bayonets were added. Having two bayonets, the torsion movement could

be blocked. But the axial displacement had to be locked too. To do so, small magnets with half of the thickness of the end rib were added to the join. They were sized with the rolling accelerations of the plane and a safety factor of 3 was applied.

3.3 Materials

The materials that have been used for the wing are various composites, two woods and one light-weighted foam. They have been selected because Trencalòs Team had already worked with them and the members had some experience. Below, the needed properties to simulate them into Abaqus are shown.

3.3.1 Carbon and glass fibers with epoxy resin

Fibers are long and thin strands of material whose diameter is between 0.005 and 0.010 mm. They are composed essentially of atoms which are bonded forming crystals in the fiber direction. These materials are characterized by having a high stiffness, low weight and high tensile strength.

The fibers are combined with a specific material called matrix and together they form the composite material. In this thesis, an epoxy resin has been used. It is the most popular thermosetting resin for FRP composites. Other members of Trencalòs Team had studied this material deeply. For more information the reader can consult [15] and [2].

At this point, the necessary properties to simulate the material are presented. Note that these are standard properties. Depending on the fiber grammage these properties could vary, unfortunately this variations depending on the weight have not been found.

Carbon and glass fiber with epoxy resin properties:

Property	Symbol	Units	Standard CF UD (0)	Standard E glass Fabric (0/90)
Density (fiber + necessary epoxy)	ρ	tonne/mm^3	1.76E-09	4.50E-10
Young's Modulus 0°	E1	MPa	135000	25000
Young's Modulus 90°	E2	MPa	10000	25000
In-plane Shear Modulus	G12	MPa	5000	4000
Major Poisson's Ratio	v12	-	0.3	0.2
Ultimate Tensile Strength 0°	Xt	MPa	1500	440
Ultimate Compressive Strength 0°	Xc	MPa	1200	425
Ultimate Tensile Strength 90°	Yt	MPa	50	440
Ultimate Compressive Strength 90°	Yc	MPa	250	425
Ultimate in-plane Shear Strength	S	MPa	70	40
Ultimate Tensile Strain 0°	Xεt	%	1.05	1.75
Ultimate Compressive Strain 0°	Xεc	%	0.85	1.7
Ultimate Tensile Strain 90°	Yεt	%	0.5	1.75
Ultimate Compressive Strain 90°	Yεc	%	2.5	1.7
Ultimate in-plane Shear Strain	Sε	%	1.4	1

Table 3.1: Standard properties of unidirectional carbon fiber and E glass fabric. Extracted from [9].

Abaqus inputs for carbon and glass fiber with epoxy resin:

Abaqus has no built-in system of units. The user has to decide which system to use between the ones in Figure 3.10. In this thesis the SI (mm) system was chosen so from now on, all the tables that correspond to Abaqus inputs are in these units.

Quantity	SI	SI (mm)	US Unit (ft)	US Unit (inch)
Length	m	mm	ft	in
Force	N	N	lbf	lbf
Mass	kg	tonne (10^3 kg)	slug	lbf s^2/in
Time	s	s	s	s
Stress	Pa (N/m^2)	MPa (N/mm^2)	lbf/ft^2	psi (lbf/in^2)
Energy	J	mJ (10^{-3} J)	ft lbf	in lbf
Density	kg/m^3	tonne/mm^3	slug/ft^3	lbf s^2/in^4

Figure 3.10: Abaqus systems of units. Extracted from [4].

Abaqus section	**Variable**	**Standard CF UD (0)**	**Standard E glass Fabric (0/90)**
Density	Mass Density	1.76E-09	4.5E-10
Elastic - Lamina	E1	135000	25000
	E2	10000	25000
	Nu12	0.3	0.2
	G12	5000	4000
	G13	5000	4000
	G23	5000	4000
Elastic - Fail Stress	Ten Stress Fiber Dir	1500	440
	Com Stress Fiber Dir	1200	425
	Ten Stress Transv Dir	50	440
	Com Stress Transv Dir	250	425
	Shear Strength	70	40
	Cross-Prod Term Coeff	0	0
Elastic - Fail Strain	Ten Strain Fiber Dir	1.05	1.75
	Com Strain Fiber Dir	0.85	1.7
	Ten Strain Transv Dir	0.5	1.75
	Com Strain Transv Dir	2.5	1.7
	Shear Strain	1.4	1
Hashin Damage	Alpha	1	1
	Longitudinal Tensile Strength	1500	440
	Longitudinal Compressive Strength	1200	425
	Transverse Tensile Strength	50	440
	Transverse Compressive Strength	250	425
	Longitudinal Shear Strength	70	40
	Transverse Shear Strength	70	40

Table 3.2: Abaqus inputs for composite materials

Comments about the inputs: Regarding the scientific article [27], G12=G13=G23 hypothesis can be assumed and in [28] we can see that these values are very similar. On the other hand, according to [29], the assumption of f^*=0 is acceptable for engineering.

The errors between simulations and experimental data are less than 10%.

3.3.2 Birch wood

Birch wood is characterized for having a high relation between stiffness and weight. As a wood it can not be considered an isotropic material. Instead, it is supposed orthotropic. When the wood is taken from the birch, it has three main directions: longitudinal, tangential and radial which are represented in Figure 3.11. Its properties depend on the direction and they are shown in Table 3.3

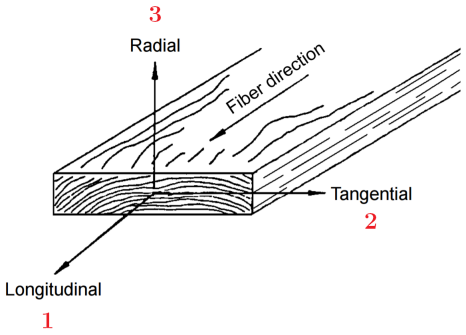

Figure 3.11: Birch wood coordinate system. Edited from [5].

Birch wood properties:

Property	Units	Value
Mass Density	g/cm^3	0.913
EL (E1)	Mpa	15290
ET (E2)	Mpa	764.5
ER (E3)	Mpa	1192.62
μLR (ν13)	-	0.426
μLT (ν12)	-	0.451
μRT (ν32)	-	0.697
μTR (ν23)	-	0.426
μRL (ν31)	-	0.043
μTL (ν21)	-	0.024
GLR (G13)	Mpa	1131.46
GLT (G12)	Mpa	1039.72
GRT (G32)	Mpa	259.93
Tension strength parallel to grain	Mpa	6.3
Tension strength perpendicular to grain	Mpa	6.3
Compression strength parallel to grain	Mpa	56.3
Compression strength perpendicular to grain	Mpa	6.7
Shear strength parallel to grain	Mpa	13

Table 3.3: Birch wood properties. Extracted from [5] and [10].

Abaqus inputs for birch wood:

Abaqus section	**Variable**	**Value**
Density	Mass Density	9.13E-10
Elastic - Orthotropic	D1111	16295.7822
	D1122	980.836993
	D2222	1137.66012
	D1133	1384.36202
	D2233	830.219713
	D3333	1788.29794
	D1212	1039.72
	D1313	1131.46
	D2323	259.93
Elastic - Fail Stress	Ten Stress Fiber Dir	6.3
	Com Stress Fiber Dir	56.3
	Ten Stress Transv Dir	6.3
	Com Stress Transv Dir	6.7
	Shear Strength	13
	Cross-Prod Term Coeff	0

Table 3.4: Abaqus inputs for birch wood

Comments about the inputs: The orthotropic values were calculated using the method explained in the section *22.2.1 Linear Elastic Behaviour* of [30].

3.3.3 Rohacell 31 IG-F

Rohacell 31 IG-F [11] is a rigid foam based on polymethacrylimide (PMI) chemistry, which do not contain any CFC's. It is characterized to have good mechanical properties with regarding its weight. It is used in automotive, aeronautical, industrial and medical industries.

Rohacell 31 IG-F properties:

Property	**Units**	**Value**
Mass Density	kg/m^3	32
Compressive Strength	Mpa	0.4
Tensile Strength	Mpa	1
Shear Strength	Mpa	0.4
Elastic Modulus	Mpa	36
Shear Modulus	Mpa	13
Elongation at break	%	3.5

Table 3.5: Rohacell 31 IG-F properties. Extracted from [11] and [12].

Abaqus inputs for Rohacell 31 IG-F:

Abaqus section	Variable	Value
Density	Mass Density	3.2E-11
Elastic - Engineering Constants	E1	36
	E2	36
	E3	36
	Nu12	0
	Nu13	0
	Nu23	0
	G12	13
	G13	13
	G23	13
Elastic -Fail Stress	Ten Stress Fiber Dir	1
	Com Stress Fiber Dir	0.4
	Ten Stress Transv Dir	1
	Com Stress Transv Dir	0.4
	Shear Strength	0.4
	Cross-Prod Term Coeff	0
Elastic - Fail Strain	Ten Strain Fiber Dir	0.035
	Com Strain Fiber Dir	0.035
	Ten Strain Transv Dir	0.035
	Com Strain Transv Dir	0.035
	Shear Strain	0.035

Table 3.6: Abaqus inputs for Rohacell 31 IG-F

Comments about the inputs: According to these scientific articles [31] and [32] the poisson's ratio can be assumed 0.

3.3.4 Balsa wood

The balsa comes from a three called Ochroma and its wood is very soft and light. It has a coarse and open grain that allows the formation of cells that are filled with air. It is very popular for light, stiff structures such as model bridges or model aircraft. As it was explained with birch wood, the balsa also have fibers (see Figure 3.12) and is considered as a orthotropic material.

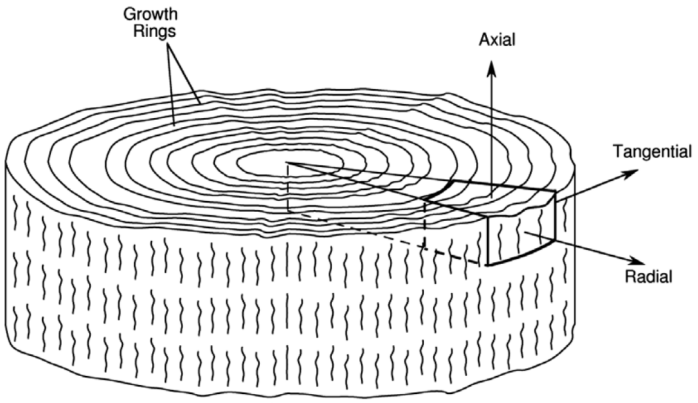

Figure 3.12: Balsa wood coordinate system. Extracted from [6].

Balsa wood properties:

Property	**Units**	**Value**
Mass Density	g/cm^3	0.287
E1	Mpa	8000
E2	Mpa	300
E3	Mpa	200
$\nu 12$	-	0.01
$\nu 13$	-	0.0075
$\nu 23$	-	0.8
G12	Mpa	350
G13	Mpa	200
G23	Mpa	2.5
Axial compressive Strength	Mpa	30.0813
Radial compressive Strength	Mpa	2.25
Shear Strength	Mpa	5.2373

Table 3.7: Balsa wood properties. The mass density has been found experimentally and the rest of variables were extracted from [13] and [14].

Abaqus inputs for balsa wood:

Abaqus section	Variable	Value
Density	Mass Density	2.87E-10
Elastic -Engineering Constants	E1	8000
	E2	300
	E3	200
	ν12	0.01
	ν13	0.0075
	ν23	0.8
	G12	350
	G13	200
	G23	2.5
Elastic -Fail Stress	Ten Stress Fiber Dir	30.0813
	Com Stress Fiber Dir	30.0813
	Ten Stress Transv Dir	2.25
	Com Stress Transv Dir	2.25
	Shear Strength	5.2373
	Cross-Prod Term Coeff	0
Hashin Damage	Alpha	1
	Longitudinal Tensile Strength	30.0813
	Longitudinal Compressive Strength	30.0813
	Transverse Tensile Strength	2.25
	Transverse Compressive Strength	2.25
	Longitudinal Shear Strength	5.2373
	Transverse Shear Strength	5.2373

Table 3.8: Abaqus inputs for balsa wood

Comments about the inputs: With regard to [33], the tensile and compressive strengths can be assumed equal.

3.4 Structural requirements

In the last section of the premises of the design, the structural requirements of the wing will be explained. The aerodynamics department of Trencalòs Team designed the wing geometry assuming that the aircraft could carry 10 Kg of payload and they made an estimation of the plane weight of 3.13 Kg. So a MTOW of 13.13 Kg was set.

When an aircraft is performing a straight and level flight the resulting lift force is equal to the airplane weight. But if it wants to turn, it has to increase its bank angle (see Figure 3.13) and the resulting loads that the structure has to bear change. To quantify

this effect, the load factor, n, is used. It is the relation between the lift that the aircraft has to generate and its weight.

$$n = \frac{L}{W} \tag{3.1}$$

There is a direct relation between the load factor and the angle of bank at which the airplane is allowed to turn. The Equation 3.2 gives us the relation and in Figure 3.13 a visual representation is shown.

$$n = \frac{1}{\cos\theta} \tag{3.2}$$

Where θ is the bank angle.

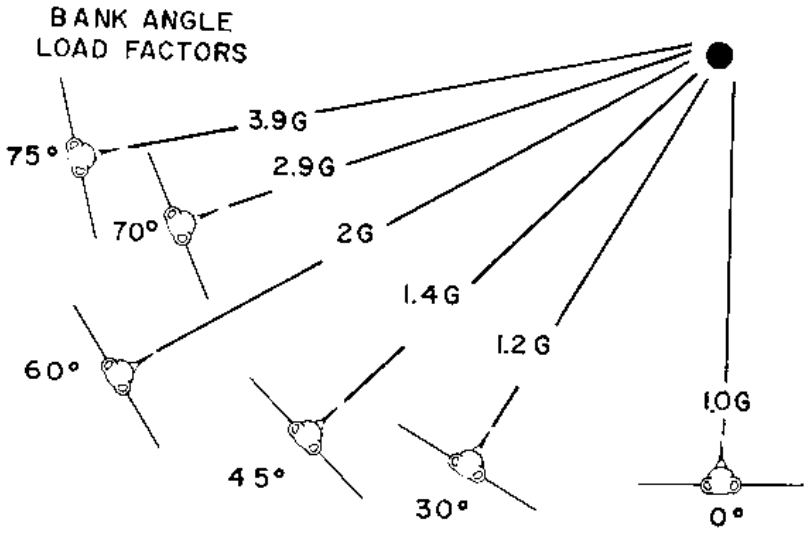

Figure 3.13: Relation between load factor and the angle of bank of an aircraft. Extracted from [7].

Trencalòs Team wanted an aircraft that could turn as fast as possible because in ACC 2017 [16] the faster the circuit was done the more punctuation the team obtained. So it was decided that the structure had to bear the forces of a load factor of 4 which corresponded to a bank angle of 75.52 degrees.

This maneuver is equivalent to a straight and level flight but with a weight of 4 times the estimated. So it was simulated this performance in XFLR5 software [34] with the 3D panels method. Figure 3.14 shows the resulting pressures on the extrados of the wing.

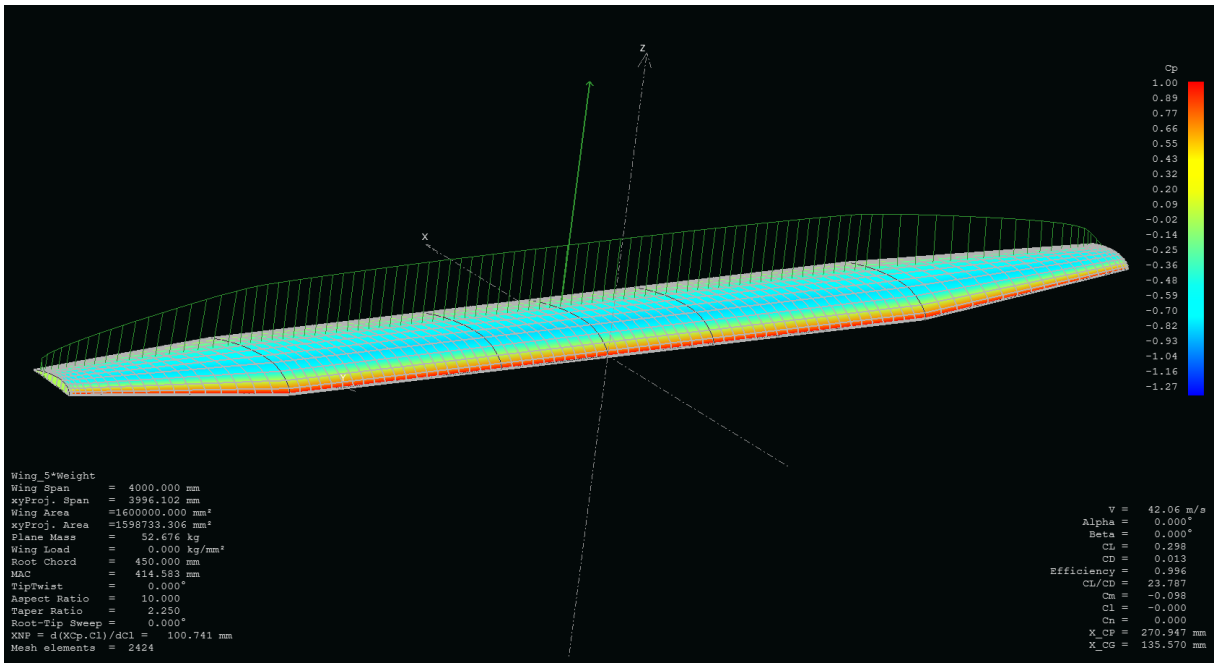

Figure 3.14: XFLR5 results of a load factor of 4.

At this point, this data had to be transferred to Abaqus. To do so, it was exported into a .txt file which included the value of pressure on each integration point of the extrados and the intrados. This information was plotted with Matlab using the script of section 2.4 of the Annexes and the result was the image of the Figure 3.15.

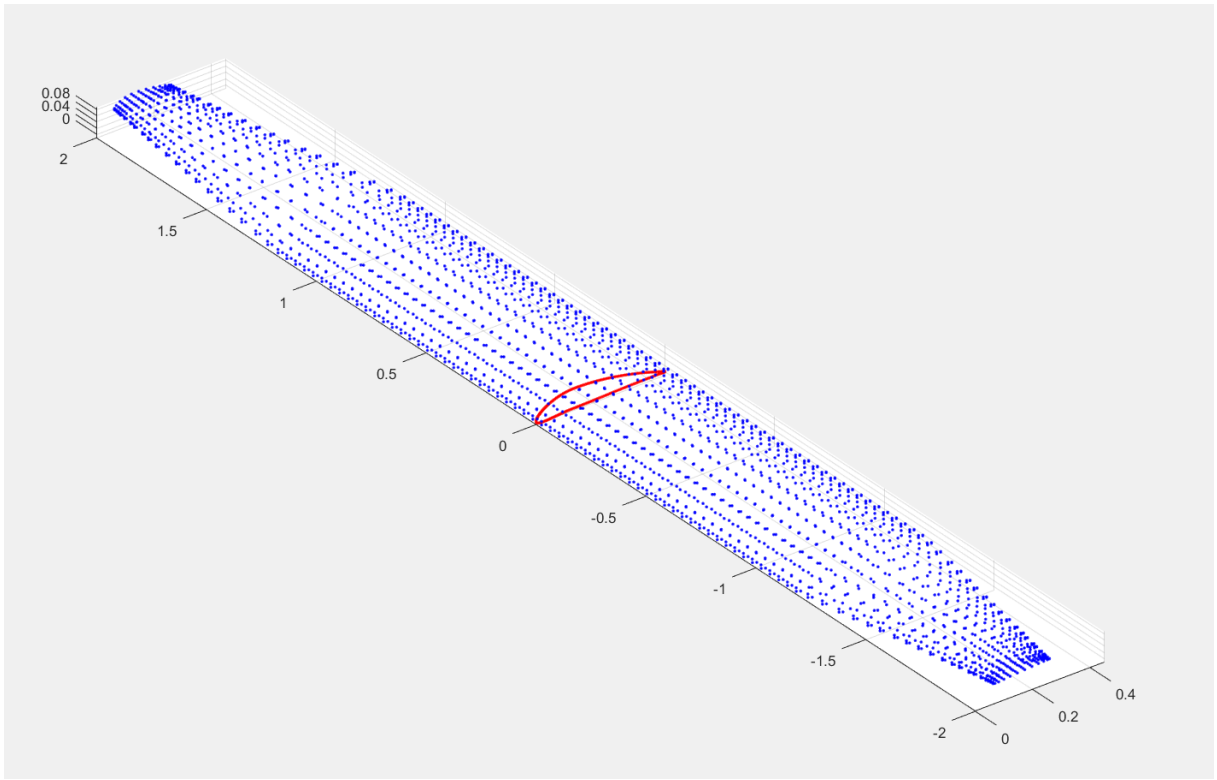

Figure 3.15: Data points from XFLR5 which contain pressure information.

Chapter 4

Failure criteria and Pareto efficiency

In order to determine whether a design breaks or not when the aerodynamic forces of section 3.4 are applied, some failure criteria will be applied. Then, if several cases pass these criteria, a tool for choosing which one is better will be needed. All of this is what is going to be explained in this chapter.

4.1 Implemented criteria

When numerical simulations of structures are done, the main results are stresses and strains which depends on the geometry and the materials of the model. However, these data is not sufficient to know whether the design bears the loads or not. To do so, some specific failure criteria must be applied. Based on the resulting data and the ultimate strength and strain of a material it is possible to predict the performance of the structure. Depending on the nature of the materials they have certain criteria. For instance, composite materials have ones that isotropic materials do not.

This thesis include different type of materials such as isotropics (Rohacell 31 IG-F), orthotropics (woods) and elastic-brittle anisotropics (composites). On the one hand, they have their own criteria which are explained in subsection 4.1.1 and on the other hand they form the entire structure which have a general stiffness matrix at which a buckling criterion is applied.

4.1.1 Static criteria

These criteria are the ones that are applied to each material. They can be classified into two groups: the ones that are implemented in Abaqus software and the ones that have been carried out by the user in the post-processing of the data. From now on, the latter

will be called custom criteria.

All them use a factor to determine if the failure has occurred or not. This value is dimensionless and is always positive. If it less than 1 then the structure is safe but if it is larger than 1 means that the structure will break. Obviously, these criteria don't represent exactly the reality because they are mathematical models. For that reason, safety factors have always to be applied to the results.

Criteria included in abaqus

They can be classified also into two groups. The ones that determine the failure mode and the ones that do not. A failure mode is the way how a structure collapse, for example shear, matrix, or fiber break.

Criteria which do not differentiate between failure modes:

These theories are the most used in engineering projects that work with structures sizing. The Abaqus user can request their values for his own simulations and the software carries out all the calculations. For more information The reader can consult the section *22.2.3 Plane stress orthotropic failure measures* of [30] and can see a comparison between these criteria in [35].

- **Maximum stress theory (MSTRS)**
  If $\sigma_{11} > 0$, $X = X_t$; otherwise, $X = X_c$. If $\sigma_{22} > 0$, $Y = Y_t$; otherwise, $Y = Y_c$.

$$I_F = max\left(\frac{\sigma_{11}}{X}, \frac{\sigma_{22}}{Y}, \left|\frac{\sigma_{12}}{S}\right|\right) \tag{4.1}$$

- **Maximum strain theory (MSTRN)**
  If $\varepsilon_{11} > 0$, $X_\varepsilon = X_{\varepsilon t}$; otherwise, $X_\varepsilon = X_{\varepsilon c}$. If $\varepsilon_{22} > 0$, $Y_\varepsilon = Y_{\varepsilon t}$; otherwise, $Y_\varepsilon = Y_{\varepsilon c}$.

$$I_F = max\left(\frac{\varepsilon_{11}}{X_\varepsilon}, \frac{\varepsilon_{22}}{Y_\varepsilon}, \left|\frac{\varepsilon_{12}}{S_\varepsilon}\right|\right) \tag{4.2}$$

- **Tsai-Hill theory [36] (TSAIH)**
  If $\sigma_{11} > 0$, $X = X_t$; otherwise, $X = X_c$. If $\sigma_{22} > 0$, $Y = Y_t$; otherwise, $Y = Y_c$.

$$I_F = \frac{\sigma_{11}^2}{X^2} - \frac{\sigma_{11}\sigma_{22}}{X^2} + \frac{\sigma_{22}^2}{Y^2} + \frac{\sigma_{12}^2}{S^2} \tag{4.3}$$

- **Tsai-Wu theory [37] (TSAIW)**

$$I_F = F_1\sigma_{11} + F_2\sigma_{22} + F_{11}\sigma_{11}^2 + F_{22}\sigma_{22}^2 + F_{66}\sigma_{12}^2 + 2F_{12}\sigma_{11}\sigma_{22} \tag{4.4}$$

Where the Tsai-Wu coefficients are defined as follows:

$$F_1 = \frac{1}{X_t} + \frac{1}{X_c}$$
$$F_2 = \frac{1}{Y_t} + \frac{1}{Y_c}$$
$$F_{11} = -\frac{1}{X_t X_c}$$
$$F_{22} = -\frac{1}{Y_t Y_c}$$
$$F_{66} = \frac{1}{S^2}$$

If the equibiaxial stress at failure (σ_{biax}) is known, then:

$$F_{12} = \frac{1}{2\sigma_{biax}^2}\left[1 - \left(\frac{1}{X_t} + \frac{1}{X_c} + \frac{1}{Y_t} + \frac{1}{Y_c}\right)\sigma_{biax} + \left(\frac{1}{X_t X_c} + \frac{1}{Y_t Y_c}\right)\sigma_{biax}^2\right]$$

Otherwise:

$$F_{12} = f^*\sqrt{F_{11}F_{22}}$$

Where $-1.0 \leq f^* \leq 1.0$. The default value of f^* is zero. For the Tsai-Wu failure criterion either f^* or σ_{biax} must be giben as input data. The coefficient f^* is ignored if σ_{biax} is given.

- **Azzi-Tsai-Hill theory [38] (AZZIT)**
The Azzi-Tsai-Hill failure theory is the same as the Tsai-Hill theory, except that the absolute value of the cross product term is taken:

$$I_F = \frac{\sigma_{11}^2}{X^2} - \frac{|\sigma_{11}\sigma_{22}|}{X^2} + \frac{\sigma_{22}^2}{Y^2} + \frac{\sigma_{12}^2}{S^2} \tag{4.5}$$

The difference between the two failure criteria shows up only when and have opposite signs.

Criteria which differentiate between failure modes:

These theories are used for composite materials in order to know how the structure breaks. If the reader wants to know more about them he can consult the section *24.3.2 Damage initiation for fiber-reinforced composites* of [30]. They have been largely used in the last decades and there are lots of scientific articles that use them (see [39, 40, 41, 42])

- **Hashin theory [43]**

  - **Hashin's fiber tensile damage initiation criterion (HSNFTCRT)**:
    If ($\widehat{\sigma}_{11} \geq 0$), the fibers are tense and its Hashin factor is:

$$F_f^t = \left(\frac{\widehat{\sigma}_{11}}{X^T}\right)^2 + \alpha\left(\frac{\widehat{\tau}_{12}}{S^L}\right)^2 \tag{4.6}$$

  - **Hashin's fiber compressive damage initiation criterion (HSNFCCRT)**:
    If ($\widehat{\sigma}_{11} < 0$), the fibers are compressed and its Hashin factor is:

$$F_f^c = \left(\frac{\widehat{\sigma}_{11}}{X^C}\right)^2 \tag{4.7}$$

  - **Hashin's matrix tensile damage initiation criterion (HSNMTCRT)**:
    If ($\widehat{\sigma}_{22} \geq 0$), the matrix is tense and its Hashin factor is:

$$F_m^t = \left(\frac{\widehat{\sigma}_{22}}{Y^T}\right)^2 + \left(\frac{\widehat{\tau}_{12}}{S^L}\right)^2 \tag{4.8}$$

  - **Hashin's matrix compressive damage initiation criterion (HSNMCCRT)**:
    If ($\widehat{\sigma}_{22} < 0$), the fibers are compressed and its Hashin factor is:

$$F_m^c = \left(\frac{\widehat{\sigma}_{22}}{2S^T}\right)^2 + \left[\left(\frac{Y^C}{2S^T}\right)^2 - 1\right]\frac{\widehat{\sigma}_{22}}{Y^C} + \left(\frac{\widehat{\tau}_{12}}{S^L}\right)^2 \tag{4.9}$$

  The symbols in the above equations have the following meaning:

  - X^T **-** Longitudinal tensile strength
  - X^C **-** Longitudinal compressive strength
  - Y^T **-** Transverse tensile strength
  - Y^C **-** Transverse compressive strength
  - S^L **-** Longitudinal shear strength

- S^T **-** Transverse shear strength
- α **-** Is a coefficient that determines the contribution of the shear stress to the fiber tensile initiation criterion
- $\widehat{\sigma}_{11}$, $\widehat{\sigma}_{22}$, $\widehat{\tau}_{12}$ **-** Components of the effective stress tensor, , that is used to evaluate the initiation criteria and which is computed from: $\widehat{\sigma} = M\sigma$. Where σ is the true stress and M the damage operator (see section 24.3.2 of [30]).

During the recent years, there have been more studies about composite materials and other criteria have been modeled. They are more complex and Abaqus does not incorporate them. If the used wanted to apply them he would have to program them in a Python subroutine. The scientific article [44] shows the most famous criteria and compares them.

Custom criteria

At these point, the evaluation of the composite materials was prepared. But the wing also had other elements such as the beam or spar and the ribs. In order to know if these parts would have bear the loads without breaking, some custom criteria were implemented in the Post-processing Python script (see section 5.4 and section 2.2 of the Annexes document).

They are also factors which indicates that the part is not broken if their value is less than 1. The first group is a set of equations that evaluate the beam or spar as a isotropic material and the second one are criteria to check the status of the wood ribs. The main difference between these criteria and the ones that are implemented in Abaqus is that the custom ones allow the user know the failure mode.

- **Beam failure criteria**

  The beam or spar has been treated as a isotropic material with specific strengths. In this thesis, Rohacell 31 IG-F has been used and their properties were presented in Table 3.5.

  - **Beam tensile damage initiation criterion (BTCRT)**
    If $\sigma_{11} \geq 0$, $\sigma_{22} \geq 0$ or $\sigma_{33} \geq 0$:

$$\text{BTCRT} = max\left(\frac{\sigma_{11}}{X^T_{beam}}, \frac{\sigma_{22}}{X^T_{beam}}, \frac{\sigma_{33}}{X^T_{beam}}\right) < 1.0 \tag{4.10}$$

  - **Beam compressive damage initiation criterion (BCCRT)**
    If $\sigma_{11} < 0$, $\sigma_{22} < 0$ or $\sigma_{33} < 0$:

$$\text{BCCRT} = max\left(\left|\frac{\sigma_{11}}{X^C_{beam}}\right|, \left|\frac{\sigma_{22}}{X^C_{beam}}\right|, \left|\frac{\sigma_{33}}{X^C_{beam}}\right|\right) < 1.0 \tag{4.11}$$

– **Beam shear damage initiation criterion (BSHCRT)**

$$\text{BSHCRT} = max\left(\left|\frac{\sigma_{12}}{S_{beam}}\right|, \left|\frac{\sigma_{13}}{S_{beam}}\right|, \left|\frac{\sigma_{23}}{S_{beam}}\right|\right) < 1.0 \tag{4.12}$$

The symbols above represents:

– X^T_{beam} **-** Tensile strength of the beam or spar

– X^C_{beam} **-** Compressive strength of the beam or spar

– S_{beam} **-** Shear strength of the beam or spar

- **Ribs failure criteria**

The ending ribs of each wing part were made of wood, which can not be considered as an isotropic material. Birch wood and balsa wood properties were presented in Table 3.3 and Table 3.7. The following criteria were adapted to their properties.

– **End rib parallel tensile damage initiation criterion (ERParalTCRT)**
If $\sigma_{33} \geq 0$:

$$\text{ERParalTCRT} = \frac{\sigma_{33}}{X^T_{rib}} < 1.0 \tag{4.13}$$

– **End rib perpendicular tensile damage initiation criterion (ERPerpenTCRT)**
If $\sigma_{11} \geq 0$ or $\sigma_{22} \geq 0$:

$$\text{ERPerpenTCRT} = max\left(\frac{\sigma_{11}}{Y^T_{rib}}, \frac{\sigma_{22}}{Y^T_{rib}}\right) < 1.0 \tag{4.14}$$

– **End rib parallel compressive damage initiation criterion (ERParalCCRT)**
If $\sigma_{33} < 0$:

$$\text{ERParalCCRT} = \left|\frac{\sigma_{33}}{X^C_{rib}}\right| < 1.0 \tag{4.15}$$

– **End rib perpendicular compressive damage initiation criterion (ERPerpenCCRT)**
If $\sigma_{11} < 0$ or $\sigma_{22} < 0$:

$$\text{ERPerpenCCRT} = max\left(\left|\frac{\sigma_{11}}{Y^C_{rib}}\right|, \left|\frac{\sigma_{22}}{Y^C_{rib}}\right|\right) < 1.0 \tag{4.16}$$

– **End rib shear damage initiation criterion (ERSHCRT)**

$$\text{ERSHCRT} = max\left(\left|\frac{\sigma_{12}}{S_{rib}}\right|, \left|\frac{\sigma_{13}}{S_{rib}}\right|, \left|\frac{\sigma_{23}}{S_{rib}}\right|\right) < 1.0 \tag{4.17}$$

The symbols above have the following meaning:

– X^T_{rib} **-** Tensile strength parallel to fibers of wood

– Y^T_{rib} **-** Tensile strength perpendicular to fibers of wood

– X^C_{rib} **-** Compressive strength parallel to fibers of wood

– Y^C_{rib} **-** Compressive strength perpendicular to fibers of wood

– S_{rib} **-** Shear strength of wood

The reason why custom criteria where implemented was because with the ones that Abaqus has it was not possible to differentiate between the failure modes of the spar and the ribs. The previous formulas were all implemented in the Post-processing subroutine which is explained later in section 5.4.

4.1.2 Buckling criteria

In order to evaluate the buckling response, the eigenvalue buckling prediction method is used. It is a procedure to estimate the critical (bifurcation) load of stiff structures with a linear perturbation analysis.

When the structure reaches a certain magnitude of load, a bifurcation appears in the force-displacement curve (see Figure 4.1) and there are more than one solution. They can be stable, neutral or unstable [8].

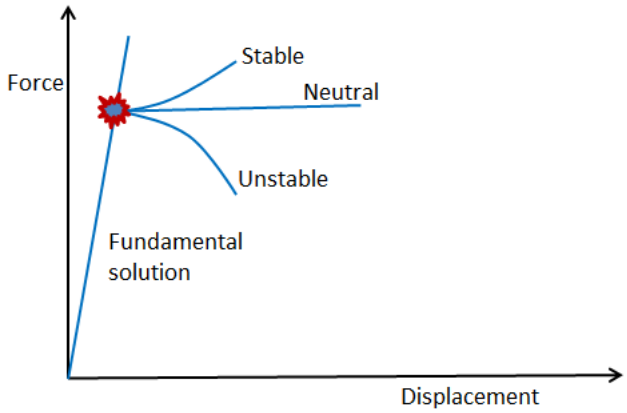

Figure 4.1: Force vs Displacement graphic of a buckling response. Extracted from [8]

In this thesis, the bifurcation point is considered as the failure criterion. So as to find it the eigenvalue problem has to be solved. It starts with the following equation:

$$K^{MN} v^{M} = 0 \tag{4.18}$$

Where K^{MN} is the tangent stiffness matrix when the loads are applied and the v^{M} are nontrivial displacement solutions. The applied loads can consist of pressures, concentrated forces, nonzero prescribed displacements, and/or thermal loading.

Abaqus is capable of solving this problem and the results are eigenvalues (λ) and their modes. If the structure was under a certain applied load, the eigenvalue is the factor by which you have to multiply the load to get to the bifurcation point. That means that if the eigenvalues are larger than 1 the structure does not experience buckling. For more information, the reader can consult the section *6.2.3 Eigenvalue buckling prediction* from [30].

4.2 Pareto efficiency

When an optimization process is performed there can be lots of variables that play a role in the design. In the structural skin of the wing, what is wanted to be optimized is the deflection of the tip, the mass, the buckling performance, the safety factor, etc.

We are ahead of a multi-variable problem [45] which is very complex. What Pareto proposed [46] was a methodology to optimize two of the variables of a design. In this thesis, the mass and the buckling performance have been selected to be optimized as it was done in [15].

The mass is a variable that we want to minimize and the buckling eigenvalues are wanted to maximize. If the buckling performance is measured with the inverted eigenvalue $(1/\lambda)$ then it has to be minimized too.

When the models in Abaqus are executed, the post-processing of the data is carried out (see chapter 5). And the results include the mass and the $(1/\lambda)$ value. If they are plotted on a graph, a point for each case is obtained. Then the a curve through the points that are minimum in mass and $(1/\lambda)$ is drawn. The result is a graphic similar to Figure 4.2.

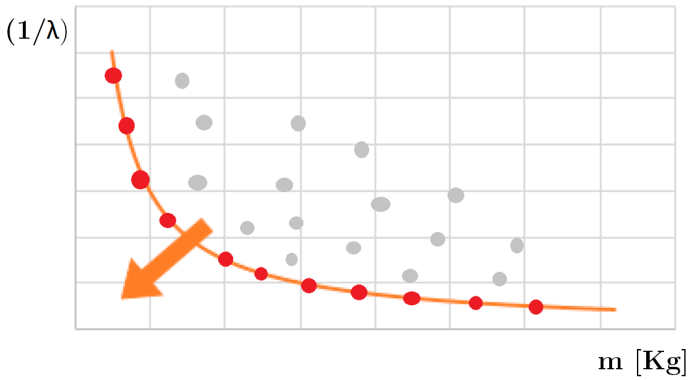

Figure 4.2: Pareto front that optimizes mass and buckling response.

This curve is called the Pareto front and it is formed by the best designs of the analyzed batch. They are optimal models that minimize both the mass and the buckling. So one of those cases will be the final design to implement in the wing structure.

Chapter 5

Design process description

5.1 Overview of the process

In this chapter the process of the design optimization is going to be explained. Firstly, an overview of the whole process will be presented with a flowchart so as to the reader can understand it.

Afterwards, the nomenclature of the folders and files used will be presented. If the reader wants to use the different codes developed in this thesis he will have to follow this codification. Finally, a detailed explanation of the different steps of the process is given. It includes the pre-processing, execution, post-processing and the Pareto efficiency.

5.1.1 Flowchart of the process

The design optimization process begins with a Starting point. It consists of a set of cases which are considered to be the initial designs to optimize. There can be as many cases as the designer wants. In this thesis, the Starting point is presented in chapter 6.

When the features of this cases are decided, the first step of the process is the Pre-processing. Here, two models in Abaqus for each case are prepared in order to simulate the responses under static and buckling loads. The extension of the resulting files will be .cae and they will contain all the information of the models.

Once all models has been prepared, the next step is to carry out their execution. To do it, a Python code has been implemented to automate the hard work of doing it manually. The results of the executions are saved in .odb files which are databases of the numerical results.

At this moment there will be tonnes of data in the results files, therefore a post-processing has to be done. It is required to select the specific information that we are interested in. This extraction is performed also using a Python code which enters to each .odb file and gets the needed items writing them in a .txt file.

After this, the best designs has to be selected performing a Pareto efficiency process. In order to do it, a MATLAB code has been elaborated. The input is the .txt file and the result is a set of optimal cases.

With the optimal Pareto front, conclusions of the Starting point can be done. These, will be the base of the new set of cases called Improvements. The features of these cases are improvements of the best results of the later models.

At this point, the same steps explained before are applied to the new group of cases. Pre-processing, execution, post-processing and Pareto efficiency are carried out. Lastly, with these results, the final design will be chosen based in the Pareto front. The ones that optimize both mass and buckling response will be the best ones. Below, in Figure 5.1, there is a flowchart representing the described process so that the reader can see it in a graphical way.

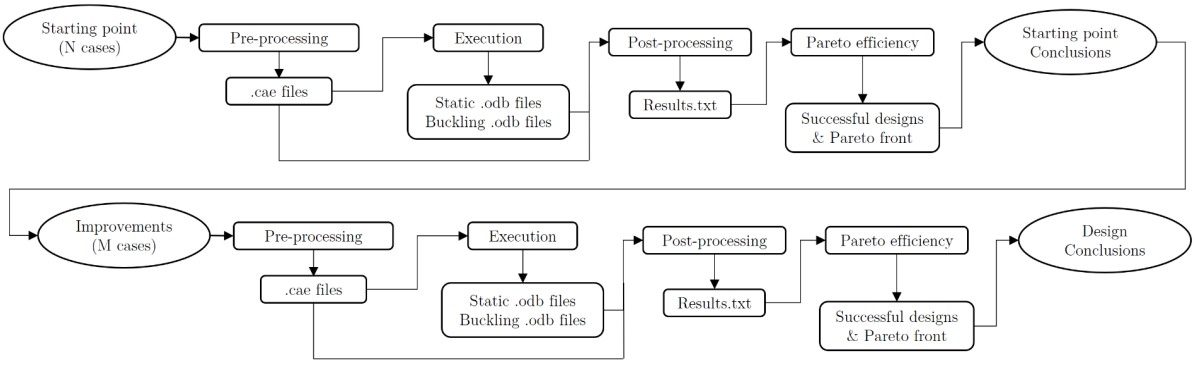

Figure 5.1: General flowchart of the design optimization process.

5.1.2 Nomenclature of the folders and files

The finality of this section is to show the nomenclature of the folders and files that has been used and to provide it to the potential readers who want to apply some of the codes of this thesis.

The main folder is named **Abaqus Simulations** and it is divided into four sub-folders:

- **MeshConvergence:** This folder contains the CATIA and Abaqus files of the convergence test that has been carried out. Figure 5.2 shows a detailed view of this folder. Each mesh model has to have its own folder named Mesh_i, where i is the number of the mesh. Inside it, there are two folders one for CATIA and another for Abaqus. The one for Abaqus has to be named Abaqus_i and its inner .cae files has to be denominated Mesh_i.

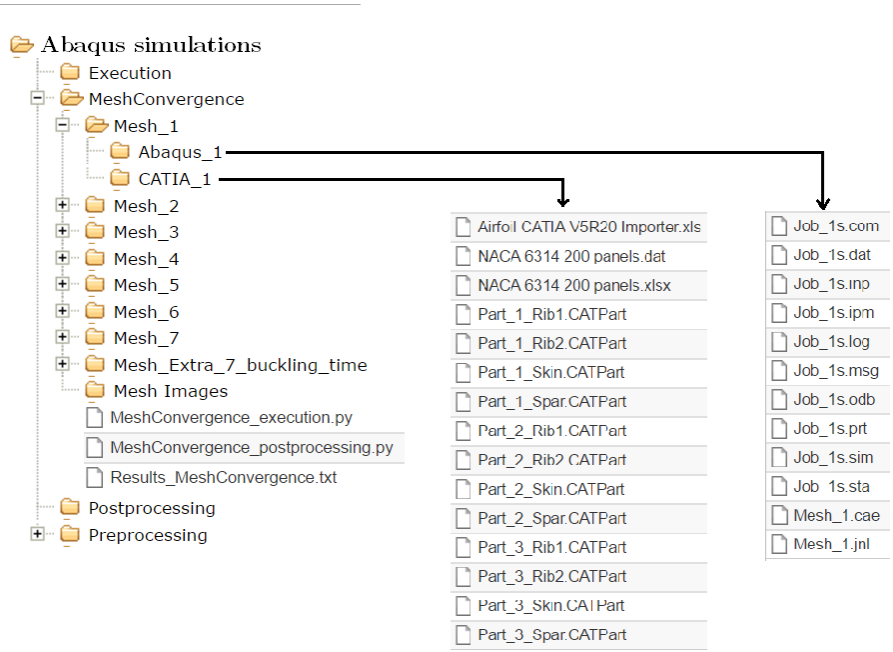

Figure 5.2: Mesh convergence folder and files.

- **Preprocessing:** Within this folder there are three more. One for the Starting point (Batch 0), another for the Improvements (Batch 1) and a last one for the needed python codes for the pre-processing of the Abaqus models. Inside a batch folder, there is one folder for each case that has to be named as Case_i, where i is the number of the case, and within it there are the CATIA and Abaqus folders. The Abaqus one must be denominated Abaqus_i and has to contain the .cae files called Case_i.

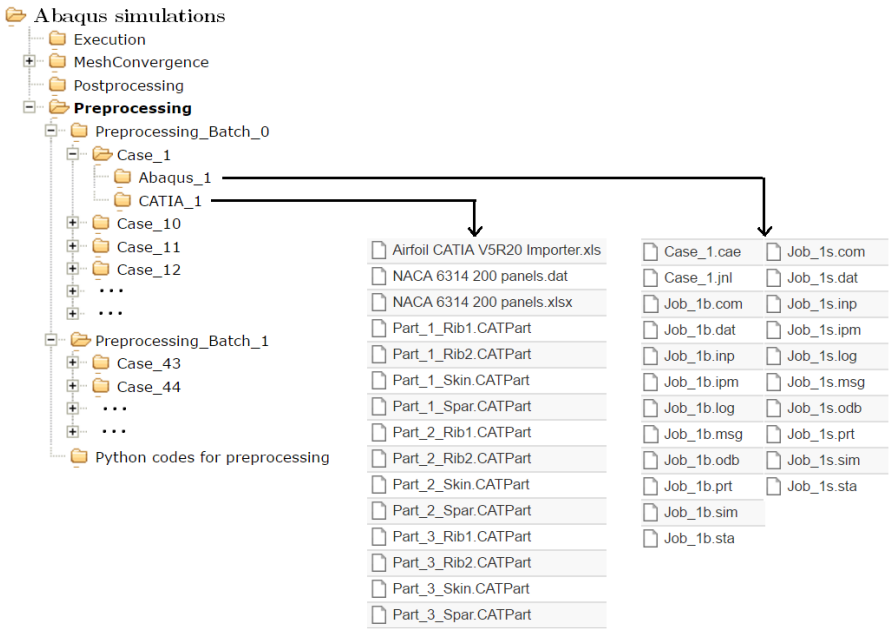

Figure 5.3: Pre-processing folder and files.

- **Execution:** Inside this folder there are only the Python codes to execute all the Abaqus models.

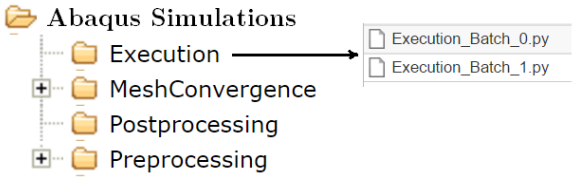

Figure 5.4: Execution folder and files.

- **Postprocessing:** The inner files are the codes for the post-procesing and Pareto efficiency steps.

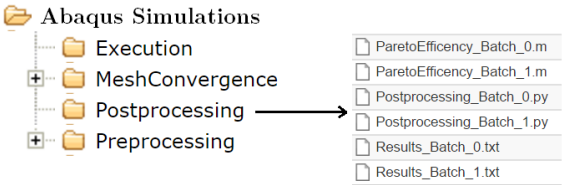

Figure 5.5: Post-processing folder and files.

Once we have covered the nomenclature of the different folders, some technical aspects are still remaining. When a Case_i.cae model database is created the user has to follow some nomenclature rules inside the file also. The static and buckling models have to be named Case_is and Case_ib respectively. Their jobs have to be also denominated Job_is and Job_ib. Finally, the Step and the Load names has to be set as Load.

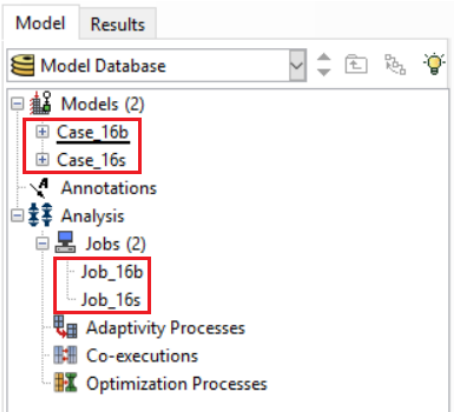

Figure 5.6: Models and jobs nomenclature.

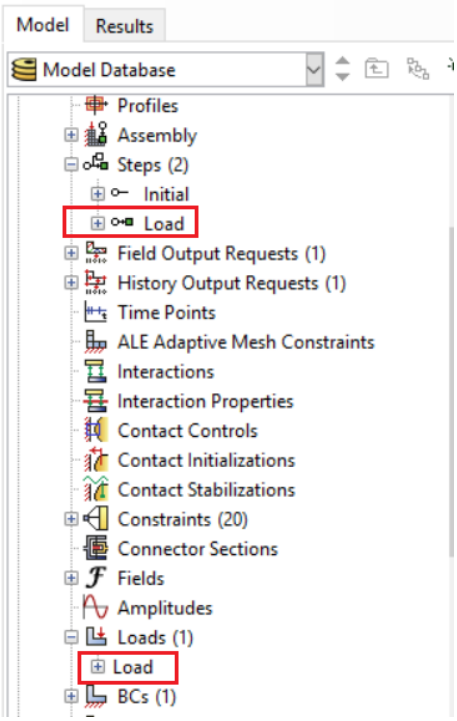

Figure 5.7: Step and load nomenclature.

5.2 Pre-processing

The first step of the design optimization is the pre-processing process. Once the features of all the desired cases has been decided, the preparation of their models has to be done. In order to do that the flowchart of Figure 5.8 will be followed.

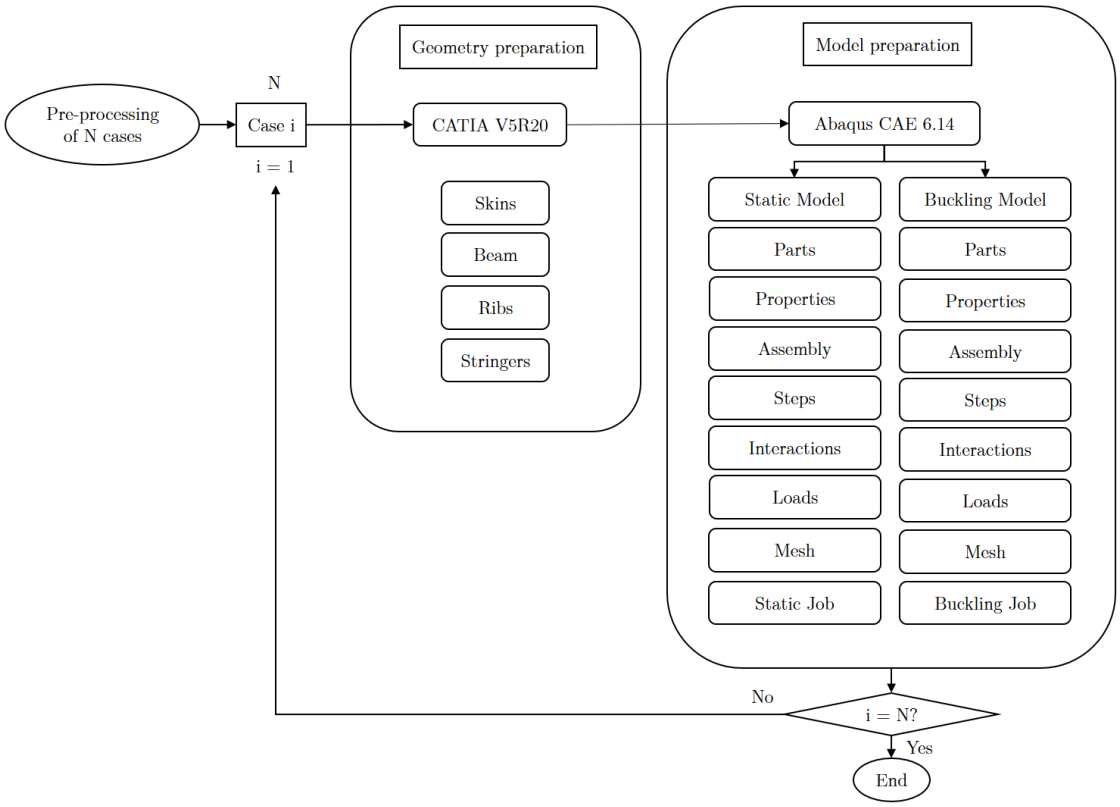

Figure 5.8: Pre-processing flowchart.

For each case, it will be necessary to do the following steps. Firstly, all the geometries of the case has to be designed. In this thesis they include the skins, the spars, the ribs and the possible stringers. At this point we have to export these geometries from CATIA to Abaqus. When the .cae file is created in Abaqus, the presented nomenclature in subsection 5.1.2 has to be applied. When the name of both the static and buckling models are set, the different geometries can be imported.
What it has to be done now is the preparation of the models. This include a series of steps that correspond to each Abaqus module:

- **Part module:** In most cases, the part module is used to create the geometries needed with its tools. But in this thesis the geometries has been imported from CATIA because of their complexity. What is has to be done is the definition of the surfaces of each part. The surfaces have to correspond to those that are going to be joins between parts. Apart from this, the sets for the encastre and for the

- **Property module:** Using this module, materials have to be created and assigned to each part. Firstly, the materials are generated according to their properties presented in section 3.3. Then, if the part is a homogeneous solid, its section has to be assigned with the corresponding tool. If the properties depend on the directions, a

material orientation has to be defined too. For the composite materials, a composite layup has to be generated with the *Create Composite Layup* tool. It is very important to define the orientation correctly. In this thesis the discrete definition has been used. The different plies of the design are filled with their material, thickness, region and rotation angle. Another crucial thing is the definition of the offset. The user has to be sure about the base plane position and the stacking direction.

- **Assembly module:** Regarding the assembly, Abaqus let the user use different tools to position the parts. But, for convenience, the dimensions of all of them and their position were defined in CATIA previously. In this way, when an instance is created in the assembly module, the part is located automatically in the right place. All the instances are created with the *Dependent* mesh option, therefore the part in the assembly has the same mesh as the individual part.

- **Step module:** In this module, it has been set up the steps and the needed output variables. The static model has to have its static step, which is called *Static, General*, and the buckling model its buckling step called *Buckle*. Besides, the *Field Output Requests* are also established. In this thesis the following outputs have been demanded:

  - For the Static model: CFAILURE, E, HSNFCCRT, HSNFTCRT, HSNMCCRT, HSNMTCRT, P, RF, S, and U

  - For the Buckling model: U

- **Interaction module:** At this point, the assembly is defined but the parts still are not joined. In order to do so the interaction module has to be used. For each join that the user wants to characterize a constraint will be applied. The *Tie* constraint type is the only that has been utilized. When they are created it is necessary a *Master* and a *Slave surface*. Here, the surfaces that were set in the Part module come into play. They will be used to assign the master in slave surfaces. This step is quite significant because it can produce lots of errors. The most important thing is that a surface can not be slave twice.

- **Load module:** Once the interactions has been set, the boundary conditions have to be assigned too. In each model there have to be two: the encastre and the load. The first one is the region where the wing is fixed and correspond to a half of the central part. All the displacements and rotations of this zone are locked. On the other hand the load that the structure has to bear was presented in section 3.4. The software XFLR5 provides us a set of points that coincide with the extrados and the intrados. Each point has associated a value of pressure and they are introduced in

Abaqus as an *Analytical Field*. Then, the load is created as *Mechanical, Pressure*. Abaqus will request a distribution and it's now when the analytical field has to be selected. Its magnitude has to be set to 1 because it is the factor by which the distribution is multiplied. An visual example of the resulting boundary conditions is shown in Figure 5.9.

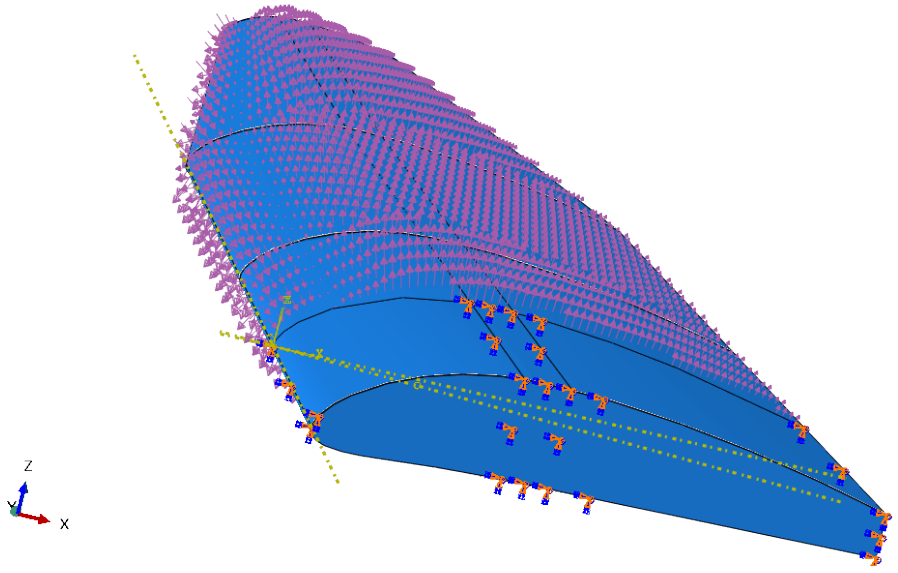

Figure 5.9: Boundary conditions of the models of this thesis.

- **Mesh module:** One of the last steps of the pre-processing process is the meshing. Each part has to be meshed individually using the tools that Abaqus provide. To mesh a part, the user has to seed it globally or by edges. Then, the mesh controls have to be chosen, including the element shape, the meshing technique and the meshing algorithm. Finally, the element type is elected and the part can be meshed.

- **Job module:** This is the last module used in the model definition process. Two jobs has to be created: one for the static model and another for the buckling one. Both have to follow the nomenclature explained in the subsection 5.1.2.

5.3 Execution

The next step after finishing the pre-processing is the execution. The labor of doing all the analysis manually was arduous. For this reason, it was decided that the best way to approach the problem efficiently was implementing a script that automatize the execution process. Abaqus uses the Python language and is able to run codes written in it.

What the script does is, for each case, open its .cae file (which contain the models) and execute the static model. Abaqus waits until it is completed and then execute the buckling one. This process is repeated for all the cases of the batch that is being analyzed. In Figure 5.10 it is possible to see the flowchart of this process.

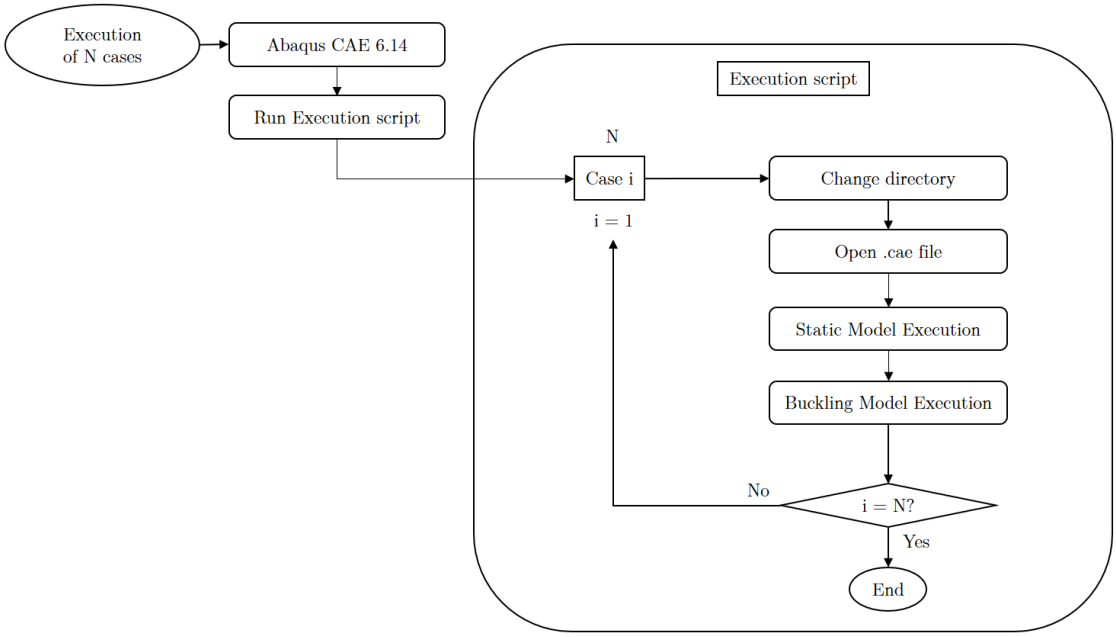

Figure 5.10: Execution flowchart.

After the running of the script, the resulting files will be created and saved each one in its corresponding Case_i folder (where i is the number case). As we saw in the subsection 5.1.1, the extension of these files is .odb and they contain all the data requested in the Step module during the pre-processing.

5.4 Post-processing

Once we have obtained all the results, we must select the information of each requested variable. If we have N cases in one batch, there will be 2N .odb files (corresponding to the static and buckling jobs). Entering to every database, picking the desired variables and finding the maximum values would have consumed a lot of time.

The optimal solution is to use a Python script as in the section 5.3. The flowchart of the post-processing process is shown in Figure 5.11 and it is explained afterwards.

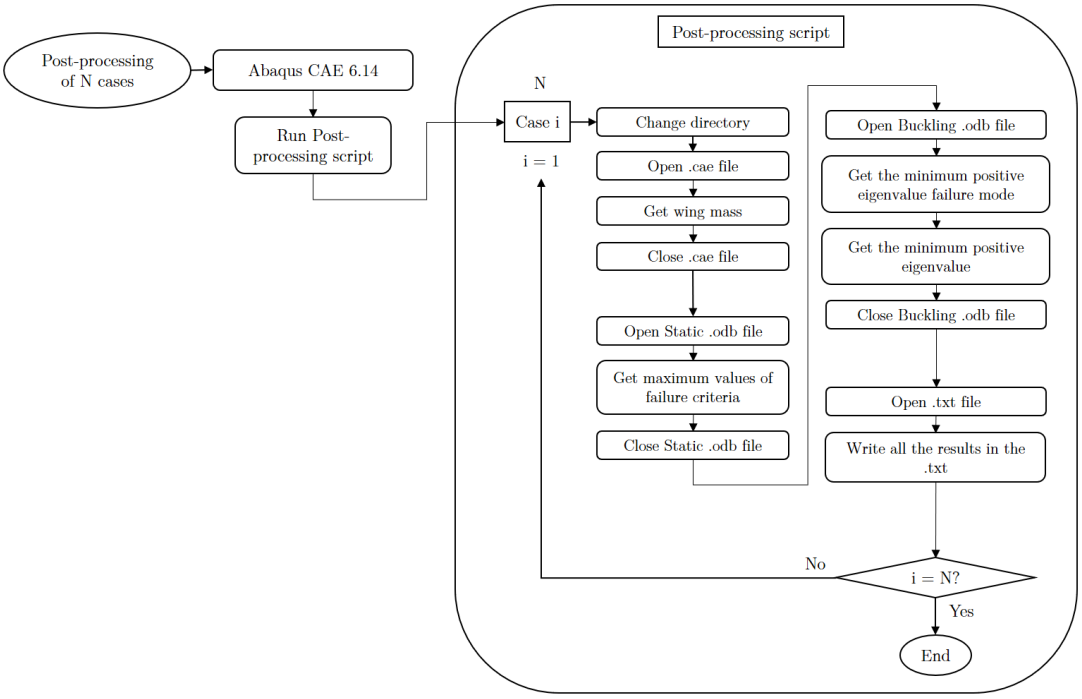

Figure 5.11: Post-processing flowchart.

The procedure starts opening Abaqus and running the post-processing script. We have to be sure that the nomenclature of subsection 5.1.2 is properly used, otherwise the code will generate errors and warnings. The .odb files both the static and the buckling have to be in their folders too. If these things are accomplished the running will perfectly work.

The code performs a general *for* through all cases because it has to extract data from all of them. It starts changing the work directory so as to open the .cae file which contains the models of the case. Then the mass of all the wing is obtained and the .cae file is closed.

The next step is to open the static .odb file which has the resulting data of the static execution. The script now gets the maximum values of the failure criteria going over all the nodes of the mesh. After this, the current file is closed. At this point, the buckling .odb file is opened. The minimum positive eigenvalue and its failure mode are extracted and the .odb is closed.

Finally, the script writes the variables of every case in a .txt file.

5.5 Failure criteria application and Pareto efficiency

The last step in the chain of the analysis of a batch of cases is the application of the failure criteria and the Pareto efficiency presented in section 4.2. To do so, a MATLAB code has been implemented in order to automatize the process too. Figure 5.12 shows us the flowchart followed while the file was done.

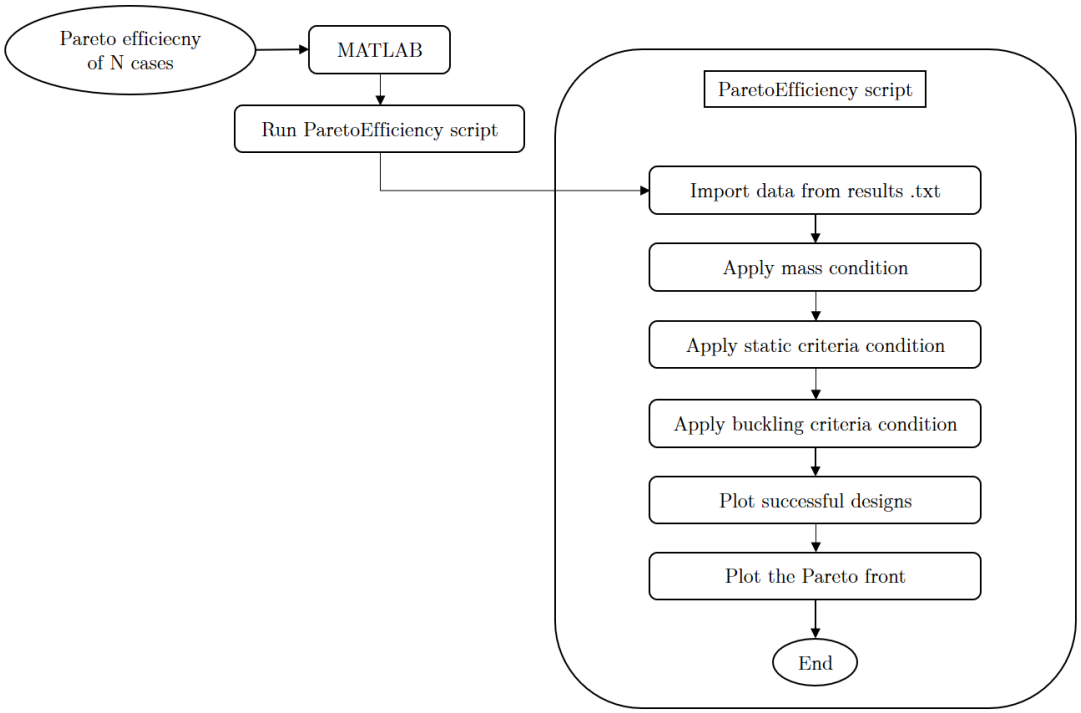

Figure 5.12: Pareto efficiency flowchart.

When the script is run in MATLAB, the data of the results is imported and saved in a table. Then the conditions are applied. The first one is a mass condition, where the user can define a maximum mass of the wing. In this thesis it has been set to 2 kg. The second one is the set of static criteria explained in subsection 4.1.1. If some design does not fulfill the criteria it is discarded. Now the buckling criterion from subsection 4.1.2 is applied. The designs that pass these conditions are saved. The last step is to apply the Pareto efficiency method. The result is a front of the cases that optimize the relation between their mass and buckling response.

With this graph, it has been possible to make the corresponding decisions in order to approach to the best design. The reader can see the Pareto diagram of the first and second batch of cases analyzed in this thesis in the section 6.4 and the section 7.3 respectively.

Chapter 6

Starting point designs

At this point, we have seen the global analysis process and detailed explanations about each step. Taking into account the premises and the requirements seen in chapter 3 the first design of the wing was considered.

As it has been explained, the wing has to fit into a box so it has to be divided in parts, specifically five. Each of them will consist of a skin made of a sandwich composite structure, a low density spar made of Rohacell IG-F 31 and two ribs of birch wood positioned at the end of each wing part to close it. It were also added some load transmission drawers with bayonets to transfer the loads from part to part.

The first idea of this structure concept was the following one. The skin was the element in charge of bearing a great part of the loads, especially the stresses due to the bending moment and the torsion of the wing. Due to the fact that it is not a good element to resist shear forces, the Rohacell spar is used to bear it while the weight did not increase very much. Two birch wood ribs were added at the end of the parts to close the structure and the load transmission drawers with bayonets were the responsible to transmit the bending moment from part to part and to block the relative rotation between them.

Regarding the simulation of the structure, some consideration were adopted. Instead of simulating the entire wing, it was carried out analysis of half of it. Looking at Figure 3.1, the central part and the two of the right were selected to be simulated. The load transmission drawers and the bayonets were not included in the simulations. They were sized using manual calculations by other members of Trencalòs Team. Thus, the parts were joined using a constraint condition between the ending birch ribs.
The boundary conditions were decided to be an encastre, which is a condition that limits all the displacements and rotations of the nodes, and the loads applied to the extrados

and intrados. In Figure 5.9 both of them can be seen.

6.1 Mesh convergence

Before choosing which structures were the ones to be optimized, a mesh convergence test was performed. It is a quite important part of every numerical analysis because the results can be very different using one mesh or another.

In order to ensure satisfactory numerical results, seven meshes were done to do the convergence test. From the first mesh to the last one, their fineness were gradually increased. In Table 6.1, it can be seen the sizes of the meshes, their number of elements and nodes and the results of the analysis. The maximum displacement (U magnitude max) was selected to be the one to compare between meshes.

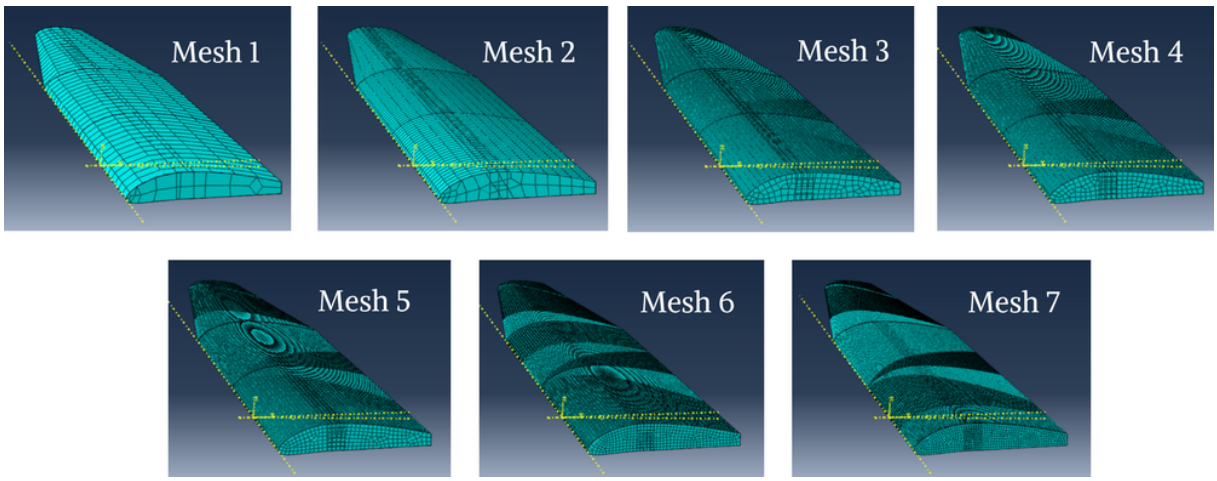

Figure 6.1: Analyzed meshes in the convergence test.

Mesh	All Parts Aprox. Global size	Part_3_Rib2 Aprox. Global size	Numer of nodes	Numer of elements	U magnitude max (mm)	Relative variation (%)
1	56	32.00	1161	911	75.31	-
2	28	16.00	3533	2929	74.22	1.45
3	14	8	13381	11684	72.69	2.06
4	12	6.86	17381	15350	72.73	0.05
5	10	5.71	26292	23360	72.64	0.12
6	8	4.57	43960	39365	72.60	0.05
7	6	3.43	83569	75820	72.55	0.08

Table 6.1: Geometrical features and results of the convergence test meshes.

At this point, the results of the test were plotted in a graph that correspond to Figure 6.2.

The X axis shows the number of nodes of the mesh which is a parameter that quantify its fineness and the Y axis represents the maximum U magnitude of the entire model.

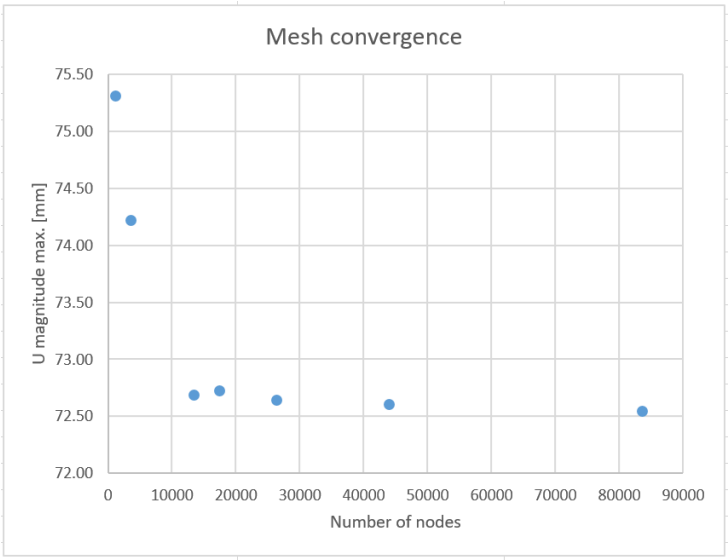

Figure 6.2: Mesh convergence results representation.

The conclusion of the mesh convergence analysis was that the relative variation of the results between the meshes was low. The objective was to find the mesh whose relative variation was below 1% so the meshes 4, 5, 6 and 7 could have been chosen. The final decision was influenced by the calculation time. Because of the analysis were static and linear, there were not much difference regarding their running time. Therefore, the mesh number 7 was selected because it was the finest.

6.2 Starting point cases

This section shows the decisions that were made after doing the mesh convergence test. As it was said in section 2.3 the main objective was to design a monocoque wing made of composite materials. But the materials and their geometries was not still decided.

The most important element was the skin. First of all, the addition of a Rohacell core idea was introduced. It was a sandwich structure that increased the inertia of the skin and gave to it more strength. The thickness of this core was decided based on the results of the reference [15], so it was set to 2 mm. Then, the density of the different fibers was searched and they showed that the addition of more than one layer on each side of the Rohacell would have resulted in a significant increment of the weight of the wing. Therefore, just one layer of fiber would be used in each side of the core.

Materials selection was the only step missing to define completely the structural skin. There were a huge amount of options that resulted of the combination of different materials and orientations. In the chapter 1 of the Annexes document of this thesis the reader can find all this combinations.

The decision of which skins analyze was influenced by various factors. Firstly, Trencalòs Team had already bought an unidirectional carbon fiber of 100 g/m^2 and the team wanted to use it. The fabrics of carbon fiber were discarded due to their expensive price. And finally it was decided to use a fabric of glass fiber to ensure a good torsion resistance.

Thus, the use a unidirectional carbon fiber and a fabric glass fiber were set. The last thing to define was their orientation and their position. The carbon fiber was decided to be through the wingspan direction to bear the stresses caused by the bending moment, while the glass fiber could be through the same direction or forming an angle of 45 degrees with it. The resulting skin combinations are shown in Figure 6.3.

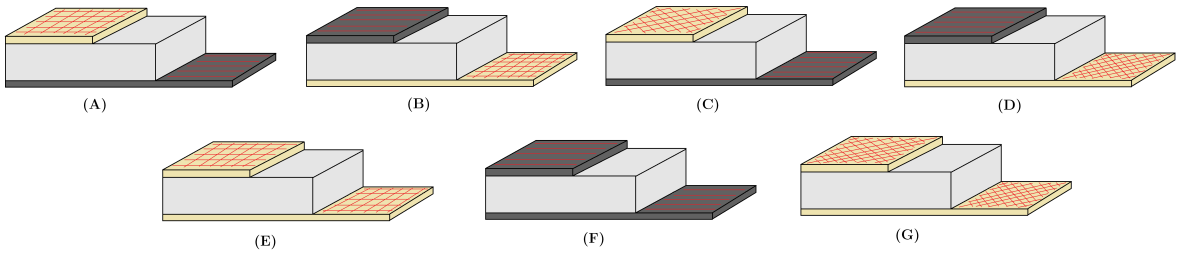

Figure 6.3: Structural sandwich skins studied in the thesis.

Regarding the spar, the sizing using manual calculations was an option but the shear load that it had to bear was not clear enough. So the best one would result from varying the spar's geometry. All of them were placed in the position that corresponded to the maximum thickness of the airfoil and different widths were established. The height of the spar was 63 mm and the widths were 10, 20, 30, 40, 50, 60 mm. The resulting spars combinations are shown in Figure 6.4.

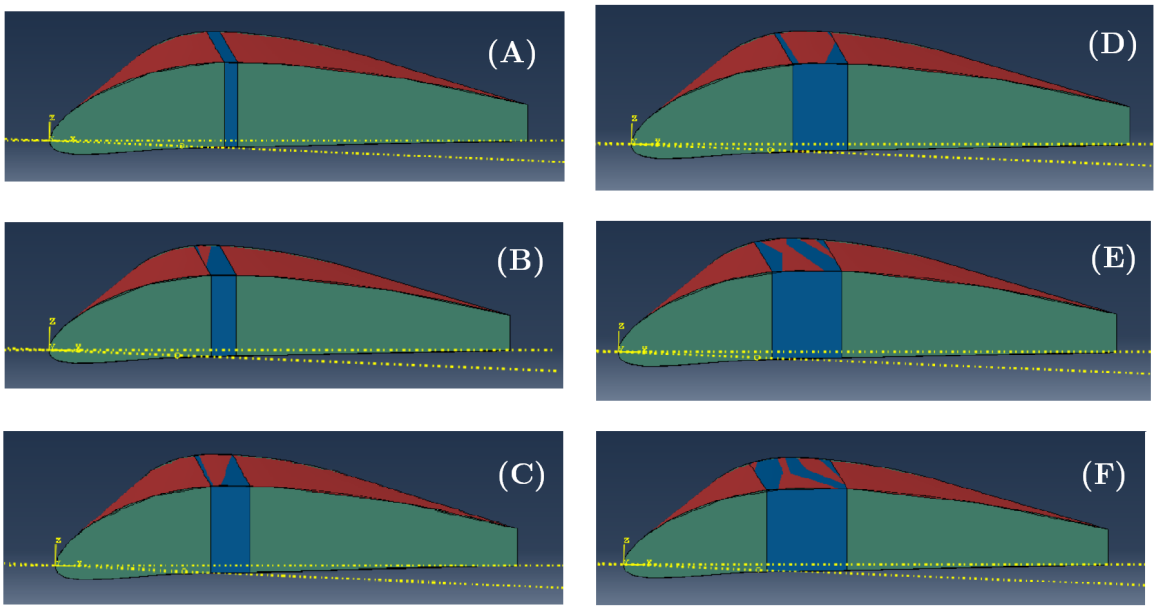

Figure 6.4: Studied spars in the Starting point batch.

At this point, we have seven skins and six spars which lead us to forty-two designs. All of them are summarized in Figure 6.5.

Batch of cases	Case	Skin (inner/core/outer) (Ply-1/Ply-2/Ply-3)	Main Spar Width [mm]
Starting Point - Batch 0	1	(0/core/0|90)	10
	2	(0|90/core/0)	10
	3	(0/core/+45|-45)	10
	4	(+45|-45/core/0)	10
	5	(0|90/core/0|90)	10
	6	(0/core/0)	10
	7	(+45|-45/core/+45|-45)	10
	8	(0/core/0|90)	20
	9	(0|90/core/0)	20
	10	(0/core/+45|-45)	20
	11	(+45|-45/core/0)	20
	12	(0|90/core/0|90)	20
	13	(0/core/0)	20
	14	(+45|-45/core/+45|-45)	20
	15	(0/core/0|90)	30
	16	(0|90/core/0)	30
	17	(0/core/+45|-45)	30
	18	(+45|-45/core/0)	30
	19	(0|90/core/0|90)	30
	20	(0/core/0)	30
	21	(+45|-45/core/+45|-45)	30
	22	(0/core/0|90)	40
	23	(0|90/core/0)	40
	24	(0/core/+45|-45)	40
	25	(+45|-45/core/0)	40
	26	(0|90/core/0|90)	40
	27	(0/core/0)	40
	28	(+45|-45/core/+45|-45)	40
	29	(0/core/0|90)	50
	30	(0|90/core/0)	50
	31	(0/core/+45|-45)	50
	32	(+45|-45/core/0)	50
	33	(0|90/core/0|90)	50
	34	(0/core/0)	50
	35	(+45|-45/core/+45|-45)	50
	36	(0/core/0|90)	60
	37	(0|90/core/0)	60
	38	(0/core/+45|-45)	60
	39	(+45|-45/core/0)	60
	40	(0|90/core/0|90)	60
	41	(0/core/0)	60
	42	(+45|-45/core/+45|-45)	60

Figure 6.5: Starting point cases of the study. The red and blue colours represent the glass fiber and the carbon fiber respectively.

6.3 Starting point results

In this section, the results of the Starting point cases (Figure 6.5) will be presented. As it has been explained in section 4.1, each case has its own static and buckling criteria. Showing all the resulting data to the reader would occupy hundreds of pages. For this reason, what it has been done is to show the visual data of the case number 1. It has been thought that it is enough to have an idea of the results. If the reader wants to see the complete numerical results, they are attached in the chapter 3 of the Annexes of the thesis.

6.3.1 Static results

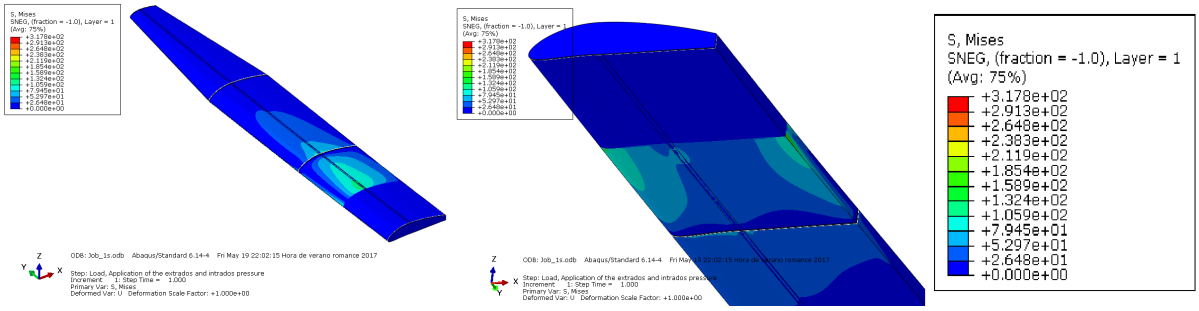

Figure 6.6: Mises stress results of case 1.

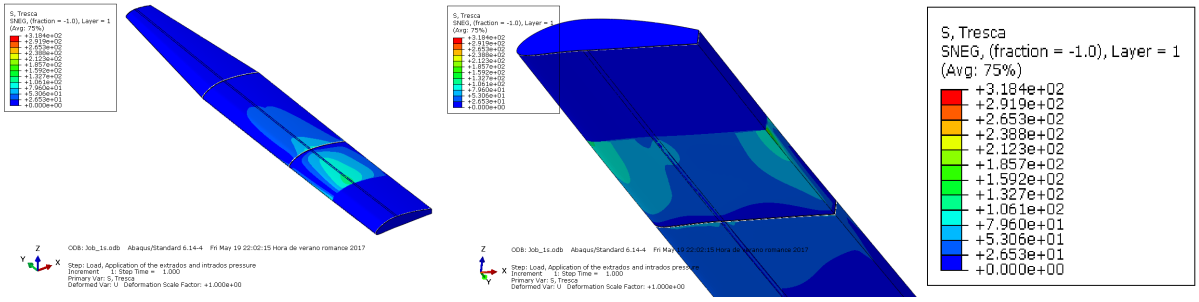

Figure 6.7: Tresca results of case 1.

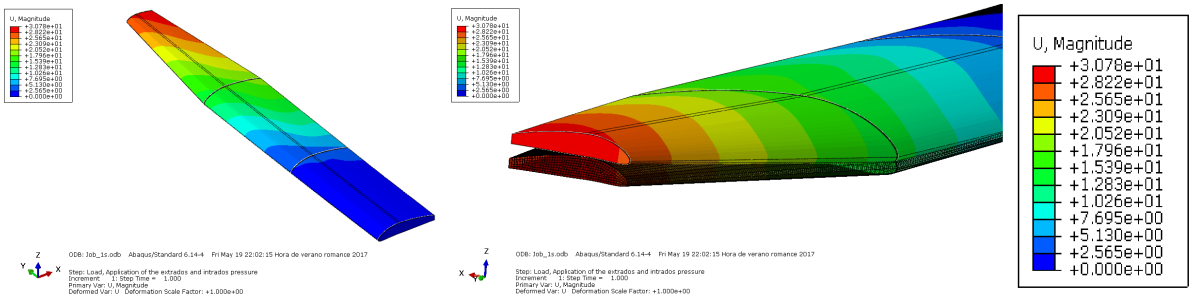

Figure 6.8: Displacements results of case 1.

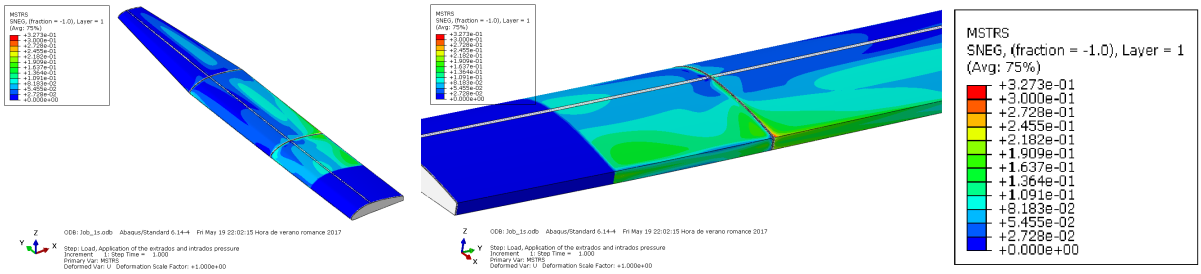

Figure 6.9: Maximum Stress criterion (MSTRS) results of case 1.

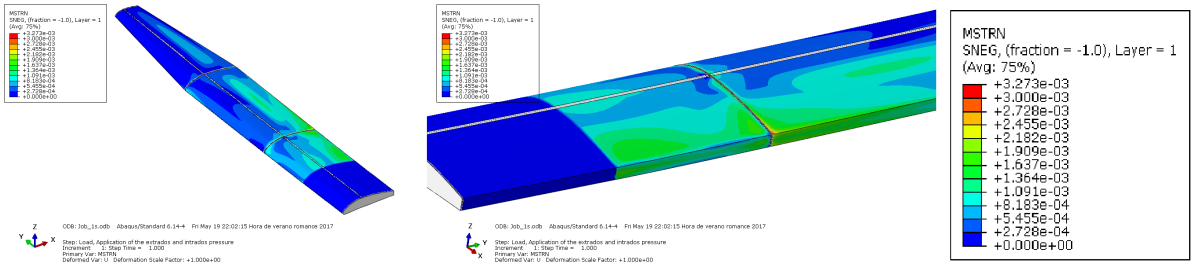

Figure 6.10: Maximum Strain criterion (MSTRN) results of case 1.

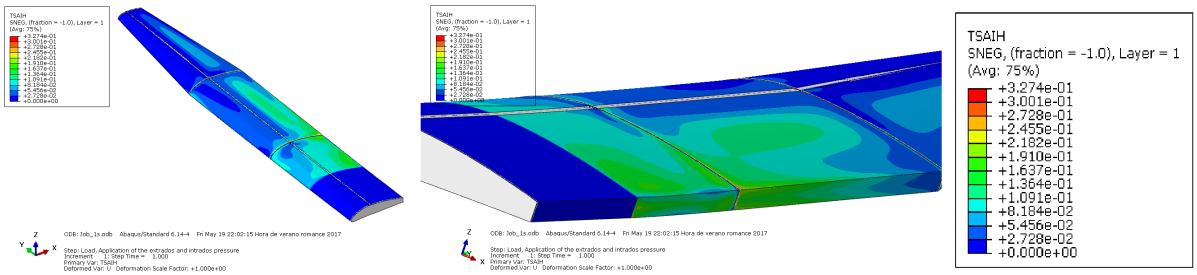

Figure 6.11: Tsai Hill criterion (TSAIH) results of case 1.

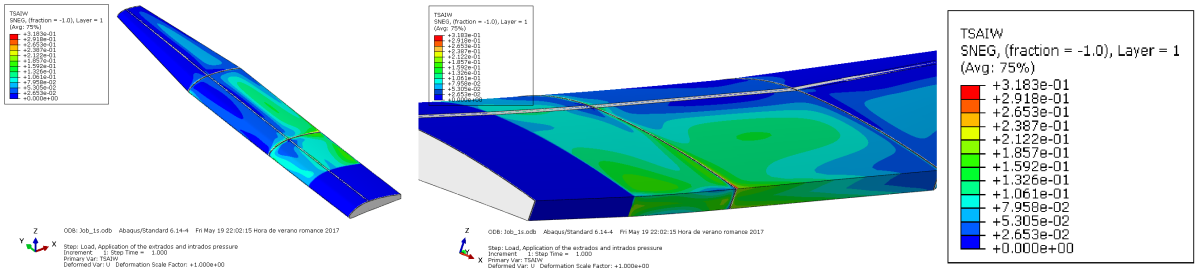

Figure 6.12: Tsai Wu criterion (TSAIW) results of case 1.

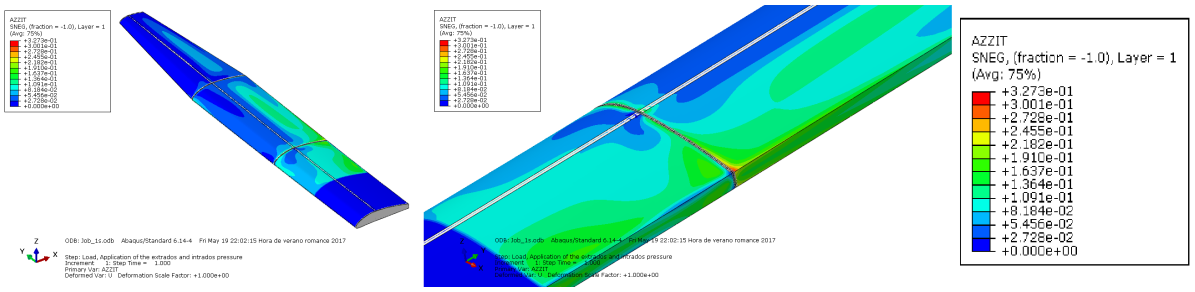

Figure 6.13: Azzit criterion (AZZIT) results of case 1.

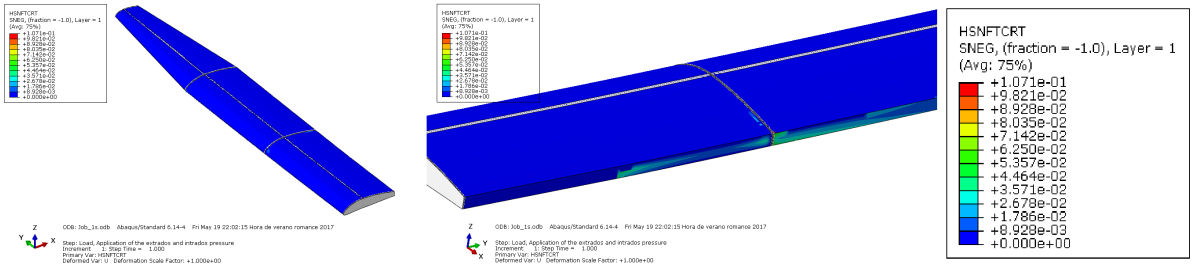

Figure 6.14: Hashin traction fiber criterion (HSNFTCRT) results of case 1.

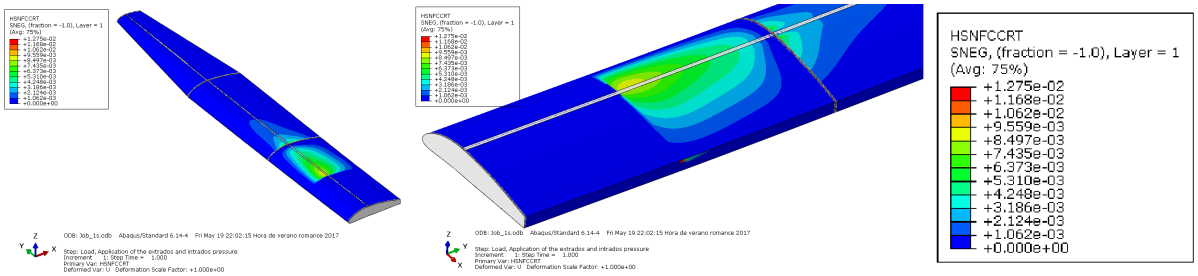

Figure 6.15: Hashin compression fiber criterion (HSNFCCRT) results of case 1.

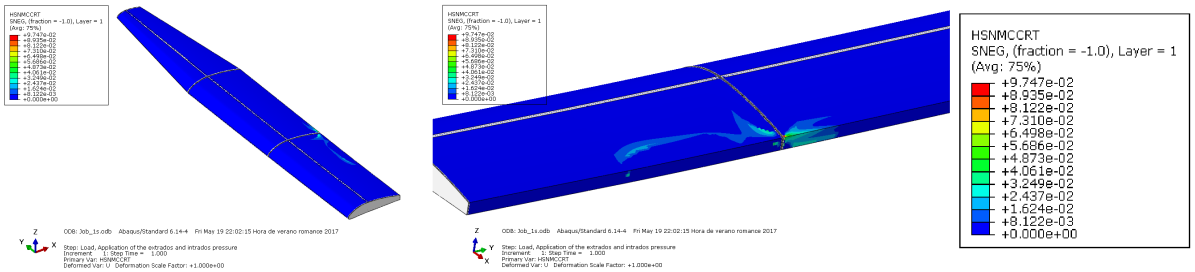

Figure 6.16: Hashin traction matrix criterion (HSNMCCRT) results of case 1.

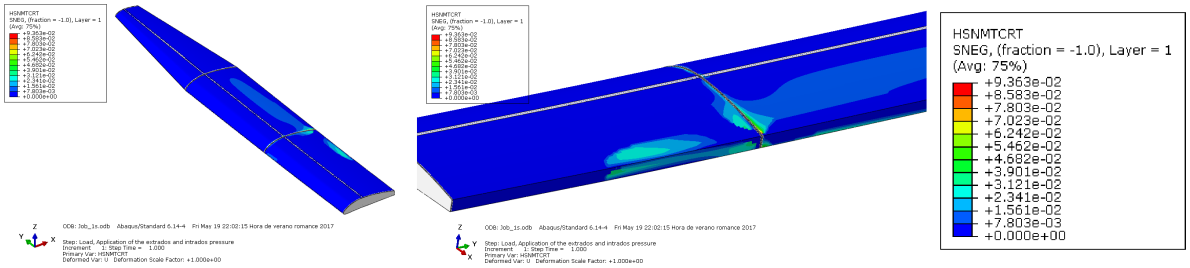

Figure 6.17: Hashin compression matrix criterion (HSNMTCRT) results of case 1.

6.3.2 Buckling results

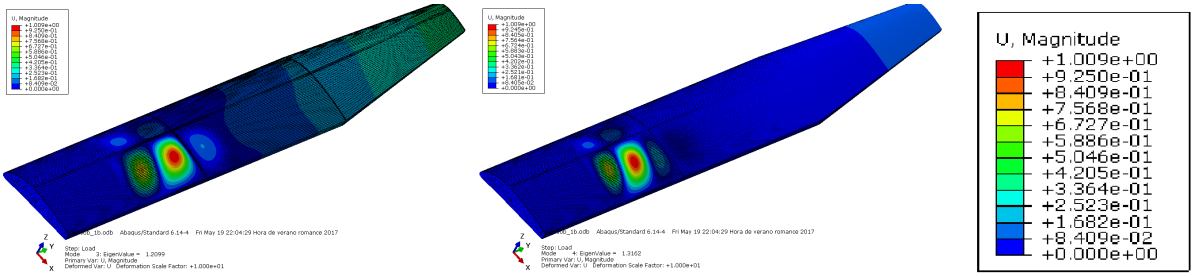

Figure 6.18: Buckling results of case 1.

6.4 Starting point conclusions

After having executed automatically the forty-two cases, their post-processing were carried out. The resulting .txt showed the maximum variables of the failure criteria and they could be compared.

The last step to accomplish the optimization of this first batch was to graph the Pareto front of our set of structures explained in section 4.2. It is a good tool to compare visually and make decisions properly. In order to do so, the script of section 5.5 was used. The result is shown in Figure 6.19.

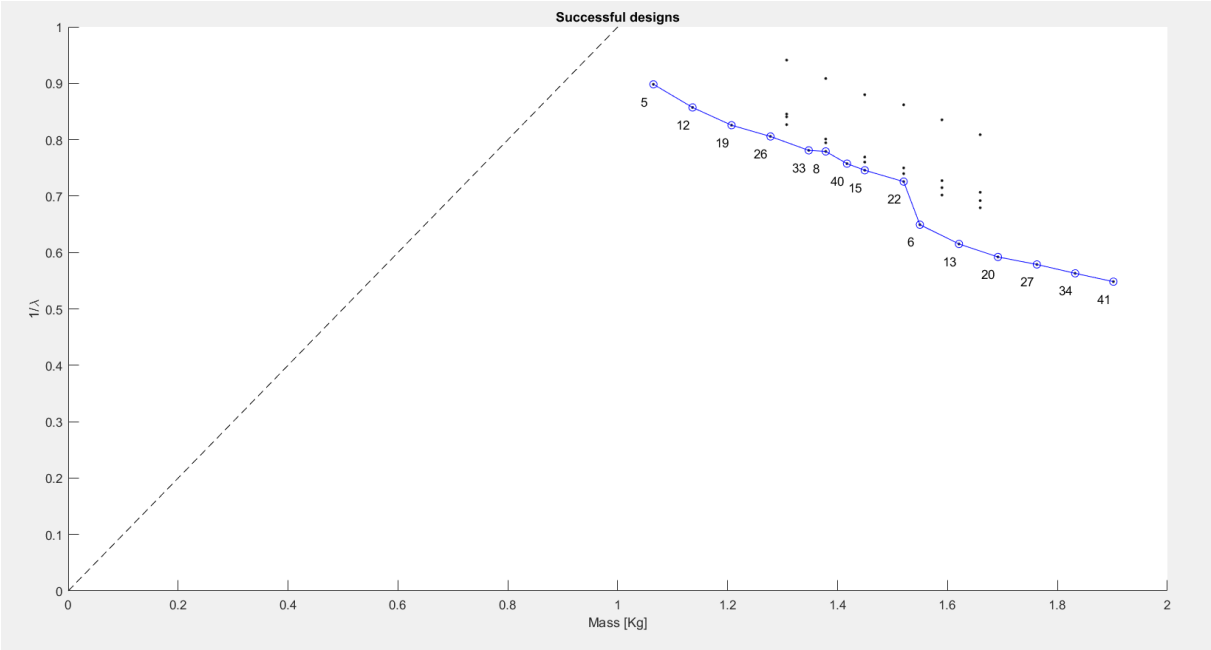

Figure 6.19: Pareto diagram of the Starting point batch.

For a load factor of 4 applied to the structural designs, the following conclusions were extracted from this information:

- All the models were expected to be more lightweight. The results show that the part that has the biggest weight is the composite skin.
- The majority of cases passed the static criteria and the maximum values of the variables were relatively low.
- The region which suffered the most was the skin of the extrados of the central part that was in compression. The zone which joins the central part with the next one was also critical.
- The maximum displacement occurred in the wingtip with values around 3 mm. It is a low value compared with the wingspan.
- According to the Hashin criteria, both the fiber and the matrix of the composite skin were able to bear the forces.
- Regarding the buckling results, they are the most critical part of the analysis. As it can be seen in Figure 6.18, a huge dent showed up on the extrados skin of the central part. Not only its dimensions were considerable but the obtained eigenvalues did not show a reasonable safety factor.
- The obtained Pareto front (Figure 6.19) presented three differentiated regions:

- **First region:** Starting from the left, we can observe the cases 5, 12, 19, 26, 33 and 40. The reader can see their features in Figure 6.5. They have a skin completely made of a fabric of glass fiber with the direction of the wingspan. This group of designs present values of $(1/\lambda)$ considerably high around 0.7-0.9.
- **Second region:** It is formed by cases 8, 15 and 22. These designs have the inner layer of the skin made of unidirectional carbon fiber and the outer of fabric glass fiber. The values of $(1/\lambda)$ are around 0.7-0.8 so they are still high.
- **Third region:** It is the right region of the curve composed by the cases 6, 13, 20, 27, 34 and 41. They have in common a skin made completely of unidirectional carbon fiber. Due to this fact, the weight of this group is considerable but on the other hand the $(1/\lambda)$ values decreased to 0.5-0.6.

Once the main conclusions were obtained, it was necessary to choose some designs so as to improve them. It has been seen that the buckling results were more critical than the static results. The Rohacell spar did not suffer so much while on the skin appeared big dents. For that reason it was conclude that the function of the spar had to change. Not only would it bear the shear forces but also prevent the buckling reducing the buckling length. It supposes a change of paradigm regarding the function of the spar.

Concerning the skins, it was decided to improve the cases of the second region of the Pareto front. The reason of this decision is that the first region has high $(1/\lambda)$ values and the models of the third one were so heavyweight. Choosing the second region was a safe decision regarding the two variables to improve, the mass and the buckling response.

All in all, the objective of the next stage was to enhance the buckling performance of the second region of the Pareto front. If this was accomplished, a design that satisfy static and buckling criteria would had been reached.

Chapter 7

Improved designs

This chapter presents the second stage of the design process showed in Figure 5.1. In chapter 6 we saw the results of the first set of designs. The main conclusions were that the buckling performance had to be improved. Thus, in the following pages some improved designs are presented.

7.1 Improved designs cases

Taking into account the conclusions of section 6.4 new models had to be thought. The cases with a 10 mm spar did bear the loads, so it was decided to use this width for the spars. It was also seen that it was not necessary that the spar was in the maximum thickness position. Instead, its position would be the best in order to reduce the buckling of the skin.

Summing up, in order to reduce the buckling failure of the structure, Rohacell ribs were added to the models and multiple spars were added to the central part which is the most critical one. Below, in Figure 7.1 the skin materials and orientations are shown. On the other hand, in Figure 7.1 the reader can see the geometrical characteristics of the new inner structures. They are differentiated by the number of ribs and spars of each part of the wing.

Batch of cases	Case	Part 1 Skin (inner/core/outer) (Ply-1/Ply-2/Ply-3)	Part 2 Skin (inner/core/outer) (Ply-1/Ply-2/Ply-3)	Part 3 Skin (inner/core/outer) (Ply-1/Ply-2/Ply-3)
Improvements - Batch 1	43	(0/core/0|90)	(0/core/0|90)	(0/core/0|90)
	44	(0/core/0|90)	(0/core/0|90)	(0/core/0|90)
	45	(0/core/0|90)	(0/core/0|90)	(0/core/0|90)
	46	(0/core/0|90)	(0/core/0|90)	(0/core/0|90)
	47	(0/core/0|90)	(0/core/0|90)	(0|90/core/0|90)
	48	(0/core/0|90)	(0|90/core/0|90)	(0|90/core/0|90)

Figure 7.1: Improvement cases features I. The blue and red colour indicate if the material is unidirectional carbon fiber or fabric glass fiber respectively.

Batch of cases	Case	Part 1 Number of 10 mm Spars	Part 1 Number of Ribs	Part 2 Number of 10 mm Spars	Part 2 Number of Ribs	Part 3 Number of 10 mm Spars	Part 3 Number of Ribs
Improvements - Batch 1	43	2	4	1	3	1	2
	44	2	6	1	3	1	2
	45	2	6	1	3	1	2
	46	3	6	1	3	1	2
	47	3	6	1	3	1	2
	48	3	6	1	3	1	2

Figure 7.2: Improvement cases features II.

The next figure shows a visual representation of the inner structures made of Rohacell of the Improvement batch.

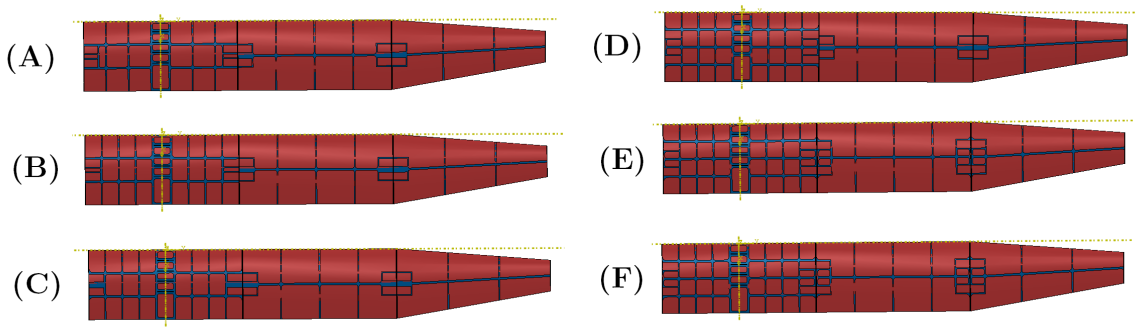

Figure 7.3: Structures for the improved designs.

7.2 Improved designs results

Once all the Improvement cases had been pre-processed in Abaqus, they were executed with the Python script presented in section 5.3. The results obtained from this step are shown in this section. As it was done in section 6.3, the static data comes first and at the end there is the buckling performance.

7.2.1 Static results

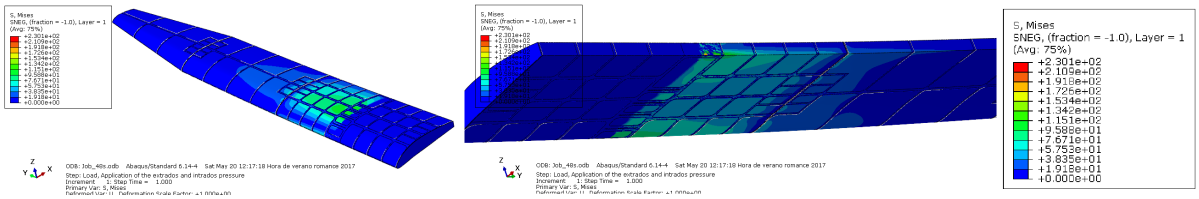

Figure 7.4: Mises stress results of case 48.

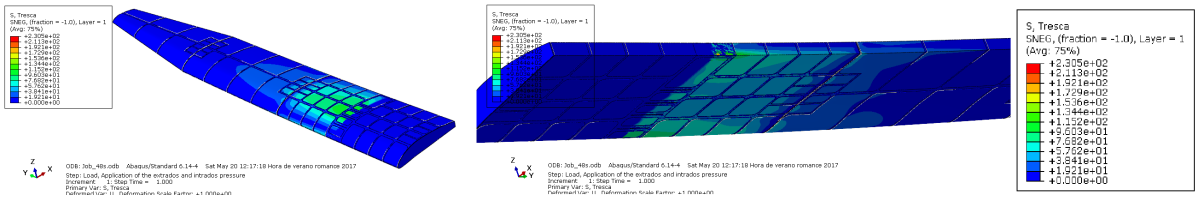

Figure 7.5: Tresca results of case 48.

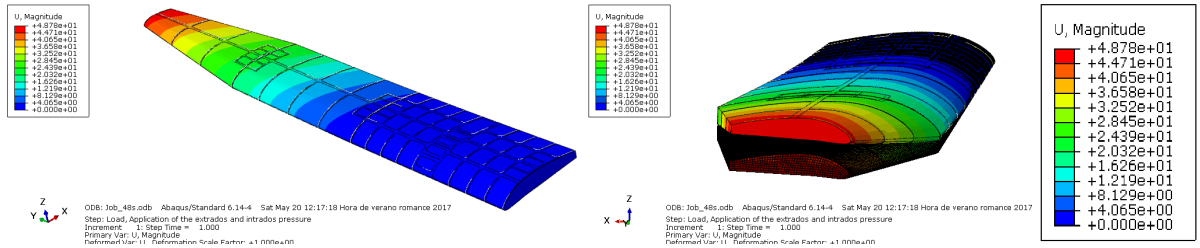

Figure 7.6: Displacements results of case 48.

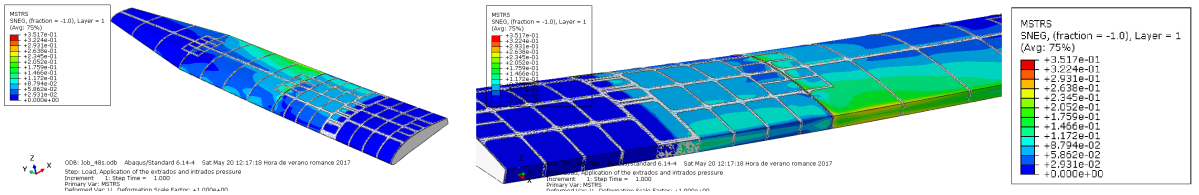

Figure 7.7: Maximum Stress criterion (MSTRS) results of case 48.

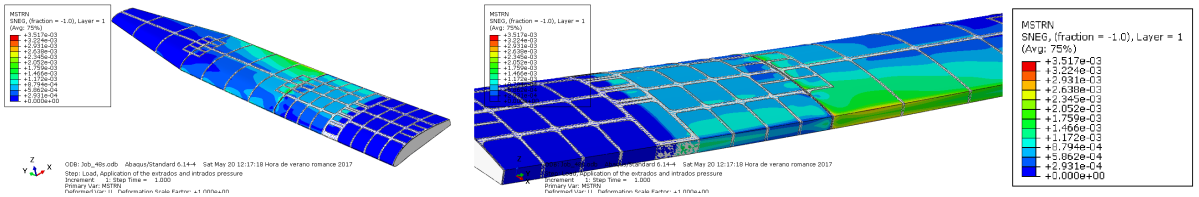

Figure 7.8: Maximum Strain criterion (MSTRN) results of case 48.

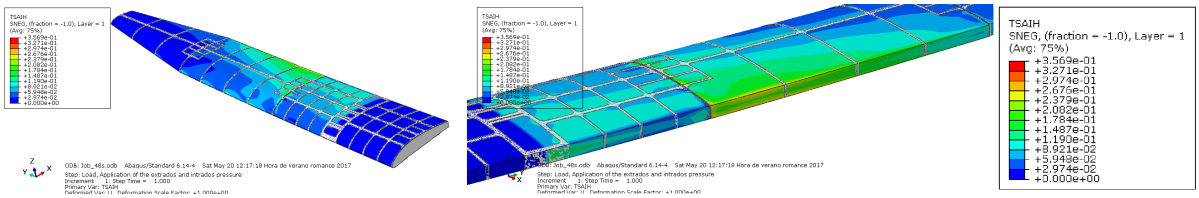

Figure 7.9: Tsai Hill criterion (TSAIH) results of case 48.

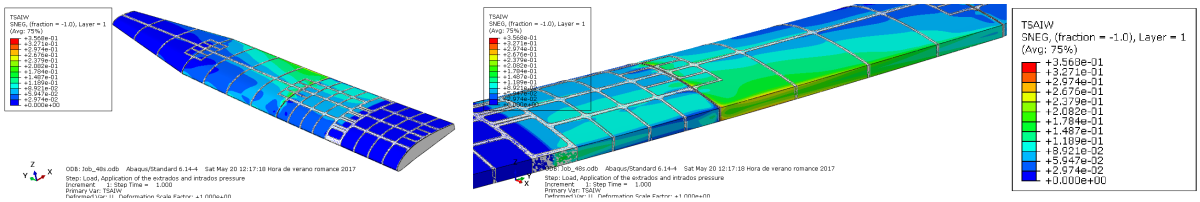

Figure 7.10: Tsai Wu criterion (TSAIW) results of case 48.

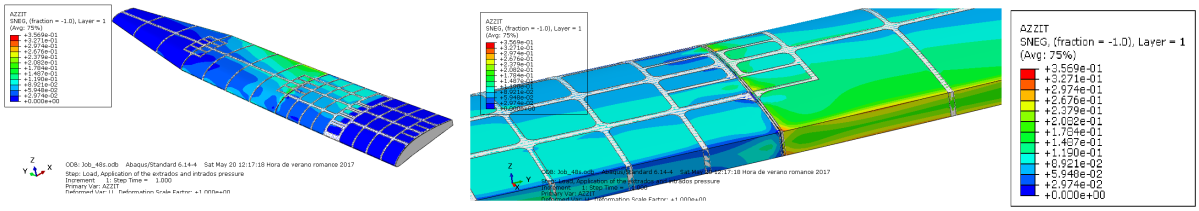

Figure 7.11: Azzit criterion (AZZIT) results of case 48.

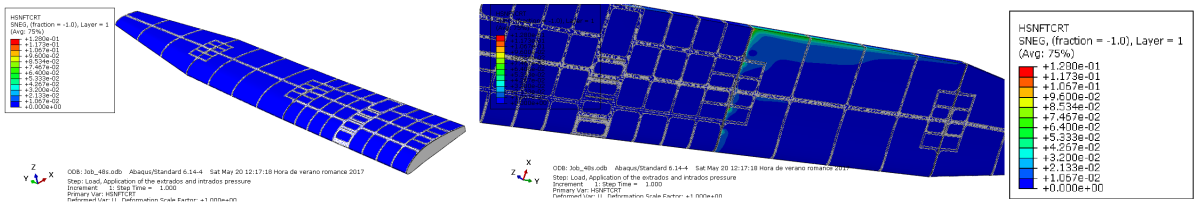

Figure 7.12: Hashin traction fiber criterion (HSNFTCRT) results of case 48.

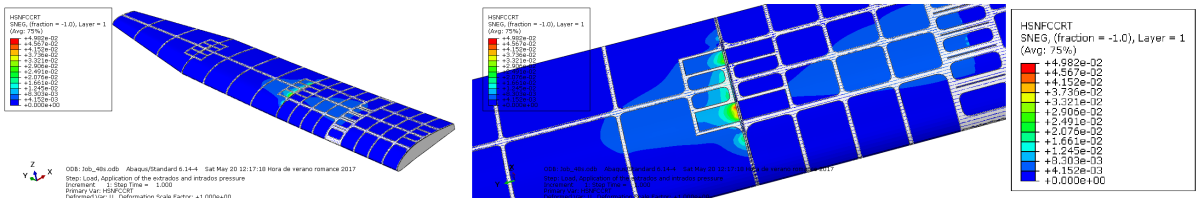

Figure 7.13: Hashin compression fiber criterion (HSNFCCRT) results of case 48.

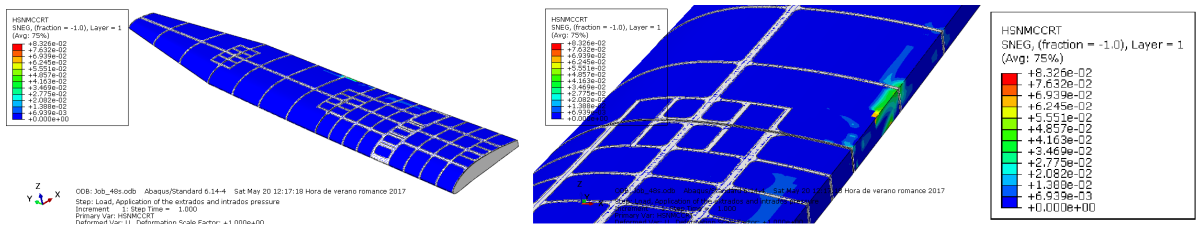

Figure 7.14: Hashin traction matrix criterion (HSNMCCRT) results of case 48.

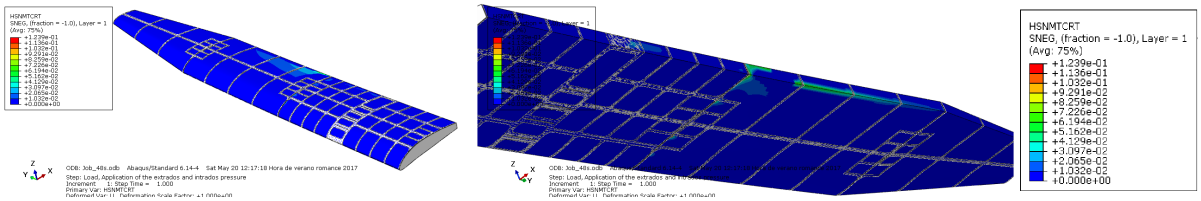

Figure 7.15: Hashin compression matrix criterion (HSNMTCRT) results of case 48.

7.2.2 Buckling results

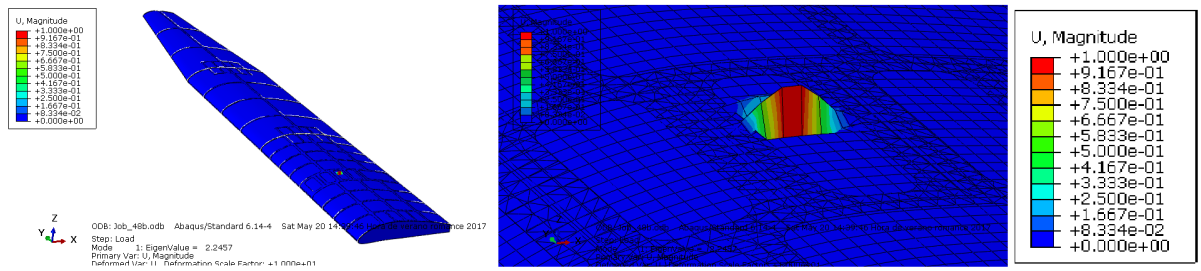

Figure 7.16: Buckling results of case 48.

7.3 Improved designs conclusions

As it has been explained in subsection 5.1.1, when we have the data corresponding to each case, the post-processing must be done. Running the script with Abaqus gives us the .txt file with the maximum values of the failure criteria. Then, it is opened by the Pareto efficiency script so as to graph the new Pareto front. The resulting graphic is shown in Figure 7.17.

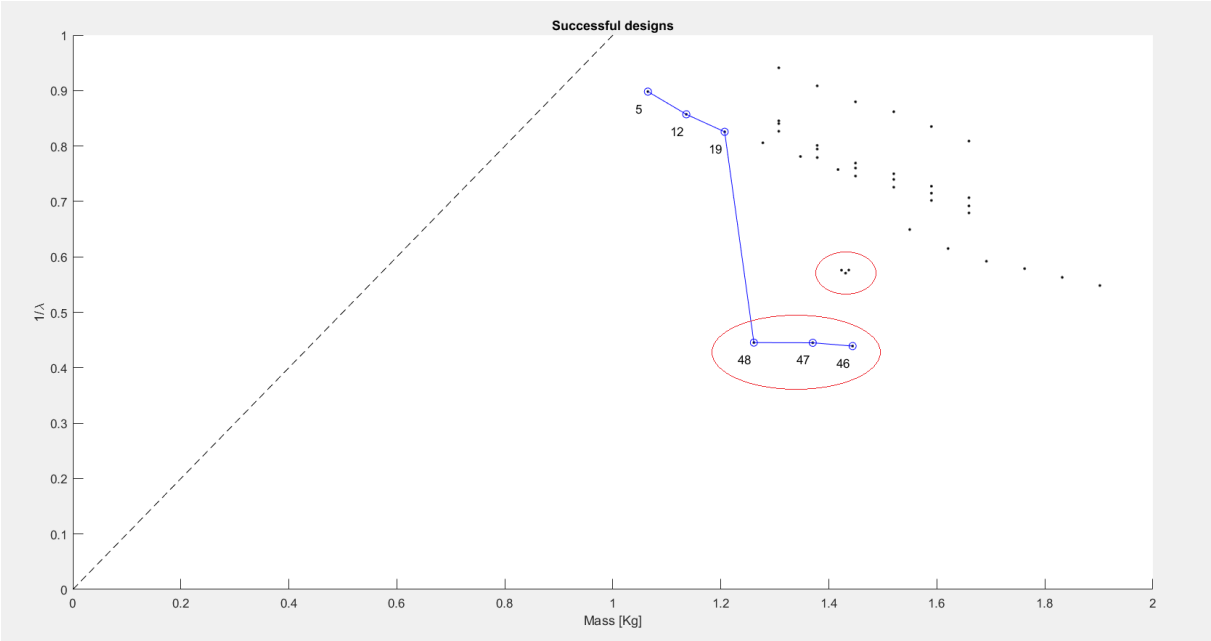

Figure 7.17: Pareto diagram of all the cases analyzed in the thesis. The improved cases have been marked in red.

According to the obtained data and the information that the Pareto diagram gives the following conclusions could be achieved:

- The mass of this batch of models did not experience big changes. This is because great part of the weight is due to the composite materials that form the structural skin. In the improvements, there just has been a redistribution of the inner Rohacell.
- All the new cases have passed the static criteria as was expected. The values are similar to the previous cases.
- The region which suffered the most has changed. In the Starting point cases it was the zone near the *encastre*, but now the critical one is near the union between the central and the next part. This could be because the inner and central structure of Rohacell distribute the loads in a better way.
- The maximum displacement was also located at the wingtip with values around 4 mm. It supposes a small increment compared with the initial cases despite this, they are still acceptable values.
- Regarding the Hashin criteria, Figures 7.12, 7.13, 7.14 and 7.15 show that now the fibers that suffer the most are the ones of the part next to the central one and that are near the join.
- Enhancing the buckling response was the main objective of this set of designs. If we observe the Pareto diagram (Figure 7.17) it is possible to see a big improvement

on the $(1/\lambda)$ values of the new models. Cases 46, 46 and 48 present the best performance with values around 0.4.

- After including the designs of the Improvement batch, the Pareto front (Figure 7.17) has changed significantly. It can be differentiated two different regions:
  - **First region:** It is formed by the Starting point cases 5, 12 and 19 and is the part of the old Pareto front that has been conserved. This is because this designs are very lightweight but they have a serious drawback. Their safety factors of buckling performance are quite low. For this reason they can not be considered the best designs.
  - **Second region:** On the other hand, we have the front formed by the Improvement cases 46, 47 and 48. This part of the curve has experienced a huge advance. The $(1/\lambda)$ results of this region has decreased down to 0.4 values keeping the same mass as their predecessors.

Having interpreted the results of the last analysis, we are now at the end of the optimization process. What is still remaining is the decision making regarding the best design. Observing Figure 7.17 there are three cases that are much better than the others in terms of optimizing mass and buckling performance. Their features are presented below in Figures 7.18 and 7.19.

Case	Part 1 Skin (inner/core/outer) (Ply-1/Ply-2/Ply-3)	Part 2 Skin (inner/core/outer) (Ply-1/Ply-2/Ply-3)	Part 3 Skin (inner/core/outer) (Ply-1/Ply-2/Ply-3)
46	(0/core/0|90)	(0/core/0|90)	(0/core/0|90)
47	(0/core/0|90)	(0/core/0|90)	(0|90/core/0|90)
48	(0/core/0|90)	(0|90/core/0|90)	(0|90/core/0|90)

Figure 7.18: Skins of the best designs in connection with mass and buckling performance optimization.

Case	Part 1 Number of 10 mm Spars	Part 1 Number of Ribs	Part 2 Number of 10 mm Spars	Part 2 Number of Ribs	Part 3 Number of 10 mm Spars	Part 3 Number of Ribs
46	3	6	1	3	1	2
47	3	6	1	3	1	2
48	3	6	1	3	1	2

Figure 7.19: Inner structure features of the best designs regarding mass and buckling performance optimization.

Chapter 8

Conclusions

In this last chapter, the conclusions of this study are discussed. There are different topics to comment so they have been divided into three sections. In the first one the conclusions about the use of the software will be reviewed. Secondly, the application of the design process exposed in chapter 5 will be deliberated and finally the optimum design will be presented and commented.

8.1 Software conclusions

First of all, CATIA software is going to be discussed. It has been used to generate all the different geometries of the simulations: skins, spars, ribs and the inner structures. In my opinion this choice has been quite right because it has tonnes of tools to create multiple geometries and shapes in a three-dimensional space. Their use had to be learn at first, but with online videos and information it has been affordable.

The second software that has been used is XFLR5. It is capable of performing aerodynamics analysis for airfoils, wings and planes operating at low Reynolds numbers. It is based on XFoil software and uses the Lifting Line Theory, the Vortex Lattice Method and a 3D Panel Method. In this thesis the latter method has been used because it gives the distribution of pressures on the extrados and intrados surfaces. Then it is imported to Abaqus and it form the load of the model. Personally, this way of defining the forces was at first confusing but when it was understood it was easy to work with.

Now we can talk about the main software of the thesis, Abaqus CAE. It is used for finite element analysis and computer-aided engineering which include static simulations (both linear and non linear), dynamic analysis, contact problems, thermal and fluid simulations, etc. Abaqus is a complete tool for carrying out structural analysis. Doing basic prob-

lems with it is an affordable task, but if the user want to do simulations similar to the reality he has to have a high knowledge of structures modelling, material properties and programming.

Another point to note is the differences between doing a single design or the optimization of a set of models. In the first case, there is a unique model to be analyzed. That means that the user could do all the process manually from the beginning to the end. But when an optimization is done, as in this thesis, the methodology changes. The definition of multiple geometries and models have to be done and depending on the case it can be a really time-consuming work. So for these cases, the whole process or part of it has to be automated. To do so, the user will have to program in Python, which is the language that Abaqus uses.

One drawback of numerical simulation models is that their results may not agree with reality. The user have to bear in mind that a model is a mathematical approximation of the real problem and there are lots of factors that may have not been taken into account. For that reason, safety factors have to be applied and the results have to be taken as a tool of comparison between models. For instance, in this thesis, two numerical software have been used: XFLR5 and Abaqus. We have to be aware of the possible error accumulation.

Regarding the use of Abaqus modules, some adversities have been found. Using the Mesh module, a few aspects were confusing such as the element types, the density mesh or the way that Abaqus calculate the results on the nodes. Defining the material properties the most difficult part was the characterization of the orthotropic ones which their properties depend on their direction. In this study they were composite materials and woods.

The methodology of this thesis is based on static and linear analysis and buckling simulations. But before setting it, some complex analysis were carried out. They were non linear simulations, damage evolution analysis, delamination modelling, and cracking propagation. They were studied because they were a better approximation to the reality. Unfortunately, their application was really difficult. It requires that the user knows high level concepts of structures and numerical simulations. Consulting documentation it was tried but the analysis were always aborted due to numerical errors and they did not converge correctly. Thus, it was decided to not include it in the scope of the thesis.

Finally, I would like to emphasize that Abaqus is a quite demanding software in terms of computer hardware. In my case, I have worked with a MSI laptop with an Intel(R)

Core(TM) i7-7700HQ CPU @ 2.89GHz processor, 16 GB of RAM and a GEFORCE GTX1050 graphic card. My experience as user is not so good because I had to work with lag when I was using the graphic interface.

8.2 Design process conclusions

In this section, the design process will be discussed. It has been based on the one that is presented on a previous thesis [15]. At first, without any knowledge of numerical methods and composite materials it was a bit overwhelming. I had to face lots of new concepts related to materials and computational calculus.

A multi-variable optimization had to be done in order to obtain the best design for the model aircraft structure. There was a great quantity of parameters to play with so the optimization had to be reduced to some geometrical features and materials.

Below, some comments and observations of each step of a batch analysis are presented according the personal experience as user.

- **Pre-processing:** As it has been explained, analyzing one of the cases of this thesis in Abaqus can be considered an easy task. But if an optimization is wanted, the user has to iterate with a huge amount of variables. All the designs combinations must be modelled in Abaqus and this is not an easy task. For every case, the geometry, the sets and surfaces, the materials, the interactions, the steps, etc. have to be defined. Even using Python codes to automate partially the modelling, it has been an arduous work and very time-consiming.

- **Programming in Python language:** During the Bachelor's degree in Aerospace Vehicles Engineering, students learn how to program scripts in various languages. But Python is not one of them and learning a new one is always challenging. The person who does it has to dedicate extra time in order to master the code syntax. Even so, in the end the files to automate some steps such as execution or post-processing have been written.

- **Programming for Abaqus:** Abaqus uses Python as base language. But if the user wants to execute processes in Abaqus he has to include some packages and libraries. Besides, he will have to learn the Abaqus commands. This software has various script guides for users who want to learn that had to be used so as to automatize the processes. The most difficult part was to understand their nomenclature because the guide had hundreds of pages.

- **Execution:** The execution stage was relatively easy. It meant a short script which entered to every case and executed its static and buckling steps. The only difficult thing was to understand the way which Abaqus language works and how it execute steps one after another.

- **Post-processing:** It has supposed the most challenging part regarding the programming aspect. First of all, various Abaqus libraries had to be used in order the code to work. Then, the Rohacell and the birch wood properties had to be defined to apply their corresponding static criteria. In addition, the mass of the models was extracted automatically and the code went over every node of the mesh finding the maximum value of each failure criterion. Finally the obtaining of the buckling data was also difficult because the data had to be parsed.

- **Programming in Matlab:** Through the degree studies, the students have learned Matlab language in some subjects such as Aerodynamics or Heat transfer. Thus, it was already known how to use the software and it was affordable. Carrying out this thesis I have learned new things like data importation or the use of table variables.

- **Pareto efficiency:** At first, the Pareto optimization concept was abstract. But when the multi-variable optimization problem was understood, this kind of optimization became clearer. It is a useful tool to visualize the results of the analysis and make decisions to reach the best design.

Lastly, note that the Improvements batch of cases has been analyzed quicker than the Starting point because all the methodology and the scripts were already made. When the user knows how to perform the analysis is much easier. Personally, I would have liked to carry out more cases and iterations, but the time was over. If I had to start now, with all the knowledge that I have learned, it would be much more bearable.

8.3 Final design conclusions

Before present the final design, a review of all the thesis will be done. The study was at first time motivated by the fact that Trencalòs Team was willing to participate in the Air Cargo Challenge 2017 event in Zagreb. The aircraft that the team would bring had to have a good design so as to compete against other international groups.

Our team wanted to have a plane made of composite materials because the majority of the previous winners had a similar design. The firs step was the aerodynamics definition

and some geometrical features such as the servos. When it was decided, the list of structural elements that could be used was identified and the materials available were set. The loads that the wing had to bear were also found with XFLR5 software and then the first conceptual design emerged.

It was a monocoque design where the main structural element was the skin made of composite materials. The addition of a spar was done because the shear forces had to be transmitted and the wing parts were joined with birch wood drawers and bayonets (see section 3.2).

After that, the use of Abaqus and the design process had to be learned, including the application of all the failure criteria and the writing of all the scripts in Python and Matlab. The next step was the definition of the static and buckling models for every case, their execution and their post-processing. This procedure was carried out twice, for both the Starting point and the Improvements batches.

In the end, a Pareto efficiency diagram was obtained for all the analyzed cases (see section 7.3). It showed us a valuable information to make a decision. All the designs that held statically were represented and the ones that formed the Pareto front were the best cases that optimized the mass and buckling performance.

At this point, the optimum design had to be chosen and it was the case number 48. In Figures 8.1 and 8.2 the reader can see its skin features and the characteristics of its inner structure.

Case	Part 1 Skin (inner/core/outer) (Ply-1/Ply-2/Ply-3)	Part 2 Skin (inner/core/outer) (Ply-1/Ply-2/Ply-3)	Part 3 Skin (inner/core/outer) (Ply-1/Ply-2/Ply-3)
48	(0/core/0|90)	(0|90/core/0|90)	(0|90/core/0|90)

Figure 8.1: Structural skin of the best design.

Case	Part 1 Number of 10 mm Spars	Part 1 Number of Ribs	Part 2 Number of 10 mm Spars	Part 2 Number of Ribs	Part 3 Number of 10 mm Spars	Part 3 Number of Ribs
48	3	6	1	3	1	2

Figure 8.2: Inner structure of the best design.

In order to help the reader have an idea of the materials and geometrical features, Figures

8.3 and 8.4 show a visual representation of the design. Both the skin and the inner Rohacell structure are exposed in the two images respectively.

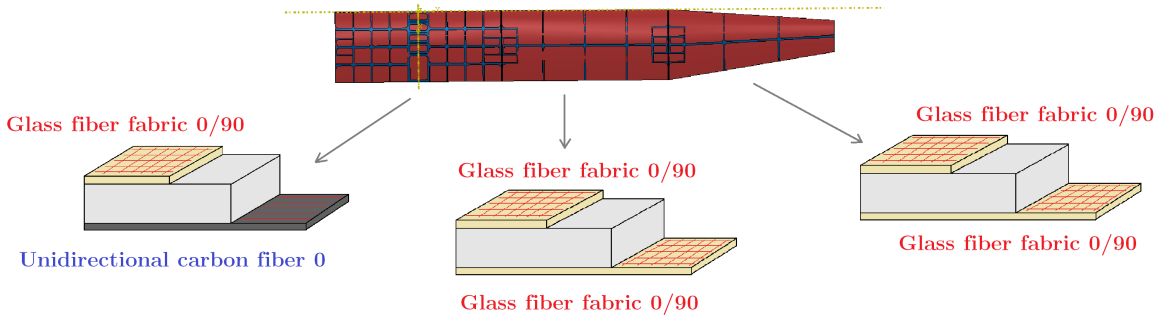

Figure 8.3: Visualization of the skin of case 48.

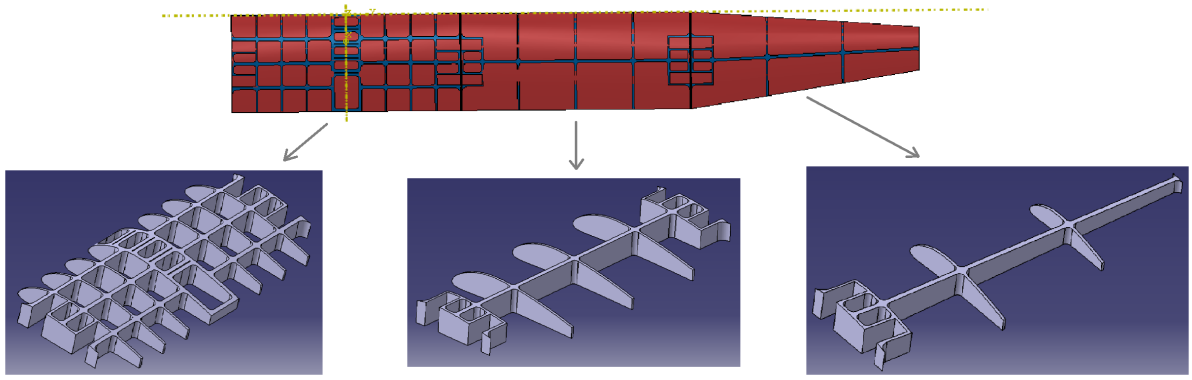

Figure 8.4: Visualization of the inner structure of case 48.

The resulting design is made of two different skins. The first one is placed on the central part and is formed by a unidirectional carbon fiber layer through the wingspan direction, a Rohacell core of 2 mm and a glass fiber fabric at the same direction. Note that the latter is the outer layer. On the other hand, the remaining parts are made (both the inner and the outer layers) of glass fiber fabric at 0/90 direction.

Regarding the inner structures, the central part has a Rohacell configuration of three spars and six ribs. It also have a central core which permits the union between the wing and the fuselage through wood frames. The second part have a single spar and three ribs and the last one has one spar and two ribs.

This case has turned out to be the best because of its results, which are presented below.

- **Mass:** 1.261 Kg (structural skin, inner structure and birch wood ribs)

- **Static performance:** The detailed results are in the chapter 3 of the Annexes of the thesis. The reader can check that all the static safety factors are above 2 so they are acceptable.
- **Buckling performance:**
  - Minimum eigenvalue of 2.2457
  - Failure Mode 1
  - $(1/\lambda)$ value of 0.4453
  - Safety factor of 2.2457

Thus, according to the results of the simulations, this structure is able to bear the forces of a 4G maneuver which means that the entire aircraft could make turns with a bank angle of 75.52 degrees.

All in all, although it is a good design it is improvable. More iterations can be done varying more parameters. For instance the implementation of different materials and orientations in specific regions of the skin where it suffers the most. For example, the addition of another layer in the leading edge, in the maximum thickness region or in the trailing edge.

Even so, I am truly proud of the work that it has been done. It has not been an easy road but I could learn so much about technical aspects of structures analysis, composite materials and the numerical methods that are currently used in important engineering projects. In a future, this knowledge will serve me in case I would like to work on some business related with numerical software and simulations

Future work

As we have seen, this thesis is a tool that can be used for the design optimization of model airplanes. The obtained design is going to be implemented in the Trencalòs Team aircraft for Air Cargo Challenge 2017. So this study can be applied to future competitions that the team will carry out.

Even so, this thesis can be developed further in different fields. They have been classified into three groups: tasks related with the material properties, with the automation of the process and with advanced techniques of simulation.

Material properties:

- Determination of all the necessary properties of the composite materials depending on their grammage. The reason of this improvement is motivated by the fact that, in this thesis, standard properties have been used and they could differ from reality. There are lots of grammages and materials (such as glass, carbon or aramid) so it could be a bachelors or masters thesis.

Design process automation:

- Automation of the pre-processing process. This would save a lot of time to the user when he wants to simulate a batch of cases.
- Automation of the whole process to perform multi-objective optimizations.

These tasks would require previous knowledge of numerical simulations, finite elements, strength of materials and a high level of Python programming skills.

Advanced analysis:

The idea would be to apply the following features to the current simulations.

- More accurate failure criteria programmed in subroutines.
- Delamination and crackling effects on composites.
- Non-linear analysis.
- Dynamic analysis.
- Simulation of the glued joins with cohesive elements.

To perform all these tasks, an engineer with a high knowledge of finite elements software, specifically of Abaqus, is needed.

Environmental and security impact

In every project or study must be a section where its environmental and security consequences are indicated. Below, the different impacts of this thesis are explained.

In relation to the environmental aspect, this thesis has both positive and negative points. Firstly, reaching an optimum design using multi-objective and multi-parametric methods can be approached by various ways. It can be done experimentally or using simulations. If the simulations method is chosen, as it was done in this study, the consequences are the following ones:

- The simulations may not be exactly as the reality, but they are approximations which can let the designer make fast decisions and discard some models. This lead to faster iterations with more designs. Thanks to it the development of composite materials can be enhanced.
- If the use of composites is increased, the resulting vehicles will weigh less and their efficiency will be improved. Thus, the engines will not have to burn so much fuel, leading to a cleaner sky and less CO_2 emissions.
- The amount of prototypes that have to be made in real life is much less than if all the cases analyzed in the simulations would be manufactured and tested experimentally.
- Less prototyping means less materials used and resources to produce them. In this aspect, it would lead to save money to the companies. The amount of materials that would have been recycled is reduced too and it supposes less pollution caused by the recycling processes.
- This study uses the computer as a work tool, which means that the main source of energy is the electricity. During the development of the thesis, lots of working hours have been needed so the consumption has been considerable. All this energy comes from mostly fossil fuel burning that emit big quantities of CO_2 to the atmosphere. This could be the drawback of the thesis environmentally talking.

Finally, regarding the security impact, the main things to be considered are related with a healthy use of the computer. The designer has to bear in mind the consequences that entail inappropriate habits. He should take into account to work in a correct position, with a straight spine posture and with the look to the front. The illumination is also a crucial point because of the eyes care and it is also recommended doing breaks from time to time.

Bibliography

[1] "Air Cargo Challenge - Wikipedia," 2017. [Online]. Available: https://en.wikipedia.org/wiki/Air_Cargo_Challenge

[2] O. Chandre, "Study of the fabrication of a monocoque structure with composites," Thesis, Universitat Politècnica de Catalunya. BarcelonaTech, 2016.

[3] G. Saran, "Study of the process of manufacture of a monocoque structure wing with composite materials," Thesis, Universitat Politècnica de Catalunya. BarcelonaTech, 2017.

[4] Abaqus Inc, "ABAQUS 6.14 GETTING STARTED WITH ABAQUS: INTERACTIVE EDITION," Abaqus Inc., Tech. Rep., 2014.

[5] United States Department of Agriculture, *Wood Handbook. Wood as an Engineering Material*. Wisconsin: USDA Forest Service, 1999.

[6] A. Da Silva and S. Kyriakides, "Compressive response and failure of balsa wood," *International Journal of Solids and Structures 44 (2007) 8685-8717*, 2007.

[7] Code 7700, "Turn Performance," 2016. [Online]. Available: http://code7700.com/aero_turn_performance.htm

[8] H. Sönnerlind, "Buckling, When Structures Suddenly Collapse," 2014. [Online]. Available: https://www.comsol.com/blogs/buckling-structures-suddenly-collapse/

[9] ACP-Composites, "Mechanical Properties of Carbon Fiber Composite Materials, Fiber / Epoxy resin (120 degree C Cure)," p. 2, 2014. [Online]. Available: https://www.acpsales.com/upload/Mechanical-Properties-of-Carbon-Fiber-Composite-Materials.pdf

[10] Matweb, "American Yellow Birch Wood," 2017. [Online]. Available: http://www.matweb.com/search/datasheetText.aspx?bassnum=PTSAP

[11] Evonik Industries, "Technical Information ROHACELL IG/IG-F," p. 2, 2017. [Online]. Available: http://www.rohacell.com/product/rohacell/en/products-services

[12] "Evonik Rohacell 31 IG Industrial Grade Polymethacrylimide (PMI) Foam," 2017. [Online]. Available: http://www.matweb.com/search/GetMatlsByTradename.aspx?tn=Rohacell%C2%AE

[13] S. Malek and L. J. Gibson, "Multi-scale modelling of elastic properties of balsa," *International Journal of Solids and Structures*, vol. 113, pp. 118–131, 2017. [Online]. Available: http://www.sciencedirect.com/science/article/pii/S0020768317300483

[14] M. Borrega and L. J. Gibson, "Mechanics of balsa (Ochroma pyramidale) wood," *Mechanics of Materials*, vol. 84, pp. 75–90, 2015. [Online]. Available: http://www.sciencedirect.com/science/article/pii/S0167663615000216

[15] M. A. Pareja Muñoz, "Study and design of a monocoque wing structure with composite materials," Thesis, Universitat Politècnica de Catalunya. BarcelonaTech, 2016.

[16] CAESA, "Air Cargo Challenge 2017 webpage," 2017. [Online]. Available: http://www.acc2017.com/

[17] "Abaqus Unified FEA - SIMULIA by Dassault Systèmes®." [Online]. Available: https://www.3ds.com/products-services/simulia/products/abaqus/

[18] "Simulation Driven Product Development — ANSYS." [Online]. Available: http://www.ansys.com/

[19] "COMSOL Multiphysics® Modeling Software." [Online]. Available: https://www.comsol.com/

[20] "MSC Nastran - Multidisciplinary Structural Analysis." [Online]. Available: http://www.mscsoftware.com/product/msc-nastran

[21] "Simulation Software — Simulation Analysis & Tools — Autodesk." [Online]. Available: https://www.autodesk.com/solutions/simulation/overview

[22] "SOLIDWORKS Simulation — Simulation Packages — SOLIDWORKS." [Online]. Available: http://www.solidworks.com/sw/products/simulation/simulation.htm

[23] "Code_Aster." [Online]. Available: http://code-aster.org/

[24] "CALCULIX: A Three-Dimensional Structural Finite Elemente Program." [Online]. Available: http://www.calculix.de/

[25] Croatian Aeronautical Engineering Student Association, "Air Cargo Challenge 2017," 2017. [Online]. Available: http://www.acc2017.com/

[26] T. Trencalòs, "Air Cargo Challenge 2015 Final Report," Universitat Politècnica de Catalunya. BarcelonaTech, Terrassa, Tech. Rep., 2015.

[27] E. J. Barbero and D. H. Cortes, "A Mechanistic Model for Transverse Damage Initiation, Evolution, and Stiffness Reduction in Laminated Composites," *Composites Part B*, vol. 41, pp. 124–132, 2010. [Online]. Available: http://barbero.cadec-online.com/papers/2010/10.1016/j.compositesb.2009.10.001.pdf

[28] D. D. Samborsky, J. F. Mandell, and P. Agastra, "3-D Static Elastic Constants and Strength Properties of a Glass/Epoxy Unidirectional Laminate," *Montana State University, Bozeman, MT 59717*, 2012. [Online]. Available: http://www.montana.edu/composites/documents/3DStaticPropertyReport.pdf

[29] R. Narayanaswami and H. M. Adelman, "Evaluation of the Tensor Polynomial and Hoffman Strength Theories for Composite Materials," *Journal of Composite Materials*, vol. 11, no. 4, pp. 366–377, oct 1977. [Online]. Available: http://jcm.sagepub.com/cgi/doi/10.1177/002199837701100401

[30] Abaqus Inc, "Analysis user's guide," Abaqus Inc., Tech. Rep., 2014.

[31] E. A. Flores-Johnson, Q. M. Li, and R. A. W. Mines, "Degradation of Elastic Modulus of Progressively-Crushable Foams in Uniaxial Compression," *Journal of Cellular Plastics*, vol. 44, no. 5, pp. 415–434, 2008. [Online]. Available: http://cel.sagepub.com/cgi/content/abstract/44/5/415

[32] E. A. FLORES-JOHNSON, Q. M. LI, and L. SHEN, "NUMERICAL SIMULATIONS OF QUASI-STATIC INDENTATION AND LOW VELOCITY IMPACT OF ROHACELL 51 WF FOAM," *International Journal of Computational Methods*, vol. 11, no. supp01, p. 1344004, nov 2014. [Online]. Available: http://www.worldscientific.com/doi/abs/10.1142/S0219876213440040

[33] T. Keller, J. Rothe, J. De Castro, and M. Osei-Antwi, "GFRP-Balsa Sandwich Bridge Deck: Concept, Design, and Experimental Validation," *Journal of Composites for Construction, ASCE, ISSN 1090-0268/04013043(10)/$25.00*, 2013.

[34] "XFLR5," 2017. [Online]. Available: http://www.xflr5.com/xflr5.htm

[35] P. P. Camanho, "FAILURE CRITERIA FOR FIBRE-REINFORCED POLYMER COMPOSITES," *Composites Science and Technology*, 2002. [Online]. Available: https://web.fe.up.pt/~stpinho/teaching/feup/y0506/fcriteria.pdf

[36] S. W. Tsai, "Strength Theories of Filamentary Structures Fundamental Aspects of Fiber Reinforced Plastic Composites," *Wiley-Interscience*, 1968.

[37] S. W. Tsai and E. Wu, "A general theory of strength for anisotropic materials." *J Composite Mat*, vol. 5, pp. 58–80, 1971.

[38] V. Azzi and S. W. Tsai, "Anisotropic strength of composites," *Exp Mech*, pp. 283–288, 1965.

[39] D. Cai, G. Zhou, X. Wang, C. Li, and J. Deng, "Experimental investigation on mechanical properties of unidirectional and woven fabric glass/epoxy composites under off-axis tensile loading," *Polymer Testing*, vol. 58, pp. 142–152, 2017. [Online]. Available: http://www.sciencedirect.com/science/article/pii/S0142941816312491

[40] G. Perillo, R. Vacher, F. Grytten, S. Sørbø, and V. Delhaye, "Material characterisation and failure envelope evaluation of filament wound GFRP and CFRP composite tubes," *Polymer Testing*, vol. 40, pp. 54–62, 2014. [Online]. Available: http://www.sciencedirect.com/science/article/pii/S0142941814001834

[41] H.-T. Hu, W.-P. Lin, and F.-T. Tu, "Failure analysis of fiber-reinforced composite laminates subjected to biaxial loads," *Composites Part B: Engineering*, vol. 83, pp. 153–165, 2015. [Online]. Available: http://www.sciencedirect.com/science/article/pii/S1359836815004758

[42] P. F. Liu, J. K. Chu, S. J. Hou, P. Xu, and J. Y. Zheng, "Numerical simulation and optimal design for composite high-pressure hydrogen storage vessel: A review," *Renewable and Sustainable Energy Reviews*, vol. 16, pp. 1817–1827, 2012. [Online]. Available: http://www.sciencedirect.com/science/article/pii/S136403211200007X

[43] Z. Hashin, "Failure Criteria for Unidirectional Fiber Composites," *Journal of Applied Mechanics*, vol. 47, pp. 329–334, 1980.

[44] P. D. Soden, M. J. Hinton, and A. S. Kaddour, "A COMPARISON OF THE PREDICTIVE CAPABILITIES OF CURRENT FAILURE THEORIES FOR COMPOSITE LAMINATES," *Composites Science and Technology*, 1998. [Online]. Available: http://www.sciencedirect.com/science/article/pii/S0266353802001252

[45] Wikipedia, "Multi-objective optimization," 2017. [Online]. Available: https://en.wikipedia.org/wiki/Multi-objective_optimization

[46] ——, "Pareto efficiency," 2017. [Online]. Available: https://en.wikipedia.org/wiki/Pareto_efficiency

About the author

Albert Herrando Moraira was born on October 8, 1995 in Santa Coloma de Gramenet, province of Barcelona, Spain. In high school, he chose the scientific-technical specialty and after doing his University Entrance Exam he decided to apply for the Bachelor's degree in Aerospace Vehicles Engineering imparted by The School of Industrial, Aerospace and Audiovisual Engineering of Terrassa (ESEIAAT).

During his studies, he evolved both personally and academically. He could learn technical knowledge of the aeronautical field and different competences very important for an engineer. This thesis supposed a big challenge for him. However, he enjoyed it and learned lots of skills such as critical thinking, self management or determination. Finishing this work, he closed an important stage of his life and started wondering what the future would hold for him.

Figure 8.5: The author, Albert Herrando Moraira